JOURNAL OF GEOPHYSICAL RESEARCH, VOL. 95, NO. B4, PAGES 4481–4499, APRIL 10, 1990

Models of Inclination Shallowing During Sediment Compaction

PORDUR ARASON AND SHAUL LEVI

Geophysics, College of Oceanography, Oregon State University, Corvallis

We construct microscopic models of compacting sediment which lead to inclination shallowing of the magnetic remanence. The models can be classified as (1) rotation of elongated magnetic grains to more horizontal orientations; (2) rotation toward the horizontal of flat nonmagnetic fabric grains to which smaller magnetic grains are attached; (3) randomization of the sediment by grain rotations which lead to decreased intensity of magnetization and possibly also to inclination shallowing; and (4) finally, we show that the initial within-sample dispersion of the magnetic moments dampens the amount of inclination shallowing of all the models and transforms any form of microscopic mechanism to an equation of a standardized form. The physically realistic models give rise to different magnitudes of inclination shallowing, which to the first order obey an equation of the form $\tan(I - \Delta I) = (1 - a\,\Delta V)\tan I$, where I is the inclination of the ambient field, ΔI is the inclination shallowing and ΔV the compaction. For these models we also calculate the effect of compaction on the intensity of magnetization, and the results show that considerable randomization is needed to offset the increased intensity due to higher concentrations of magnetic particles caused by compaction. If random rotations of the grains are biased toward rolling about horizontal axes and the randomization is sufficient to cancel the effect of greater concentrations, then the random grain rolling due to the compaction would give rise to considerable inclination shallowing.

Introduction

Anomalous shallowing of the magnetic inclination with depth in deep-sea sediments has been noted in several studies, and it has been suggested that the observed shallowing is due to compaction of the sediment [e.g., *Morgan*, 1979; *Kent and Spariosu*, 1982; *Tauxe et al.*, 1984]. The inclination shallowing has been associated quantitatively with the sediment porosity in clays from the Northwest Pacific ocean [*Arason and Levi*, 1986] and in carbonates from the North Atlantic ocean [*Celaya and Clement*, 1988]. Furthermore, laboratory experiments have demonstrated that compaction of sediment can lead to inclination shallowing in redeposition of natural deep-sea silty clays [*Blow and Hamilton*, 1978] and in synthetic sediment composed of kaolinite and magnetite [*Anson and Kodama*, 1987]. *Verosub* [1977] reviewed the important processes in the magnetization of sediments.

The probable occurrence of inclination shallowing in some sediments is of great significance and concern for paleomagnetism with respect to the tectonic and geomagnetic interpretations of remanent magnetism. North-south translations of plates, microplates, and terrains as well as tilting of blocks are deduced from remanent inclinations of sediments. Alternatively, information about the paleomagnetic field, such as the correctness of the geocentric axial dipole hypothesis, and secular variation including polarity transitions have been derived from sediments. In all these applications it is assumed that sedimentary processes such as compaction do not alter the primary remanence direction. The development (circa 1978) of the Hydraulic Piston Coring system for the Deep Sea Drilling Project (DSDP) and subsequently Ocean Drilling Program (ODP) provides means of obtaining undisturbed marine sedimentary sections of up to 200 m in length, at present, with good global coverage. To be able to utilize fully this growing body of data, it is crucial to understand and account for compaction-related effects on the remanent magnetism in sediments.

Paper number 89JB03299.
0148-0227/90/89JB-03299$05.00

Available models that predict shallowing of the magnetic inclination due to sediment compaction were derived intuitively and by analogy with mechanisms for inclination shallowing in noncompacting environments, and they were designed to fit specific observations, but they lack physical rigor. The detailed behavior of remanent magnetism in compacting environments is complex and probably never fully known. It would therefore be valuable to be able to simulate the compaction effects on remanent magnetism with a simple model(s). We present here simple but physically plausible mechanical models that cause inclination shallowing during compaction. For the proposed microscopic mechanisms we derive exact mathematical expressions which relate the inclination shallowing to sediment compaction.

Definitions

The terms inclination shallowing and compaction will be used extensively in this paper, so a brief description of them is appropriate.

Inclination Shallowing

Inclination shallowing, ΔI, is taken as the difference between the initial magnetic inclination and the inclination after compaction. Inclination changes toward lower absolute values (more horizontal) are taken as positive inclination shallowing. In this article we only consider positive inclinations, but due to symmetry the conclusions are fully valid for negative inclinations. However, the equations may have some ambiguity concerning negative inclinations, due to the way inclination shallowing is defined with use of absolute values. The inclination shallowing is sometimes called inclination error, and, its negative value, inclination anomaly.

Compaction

As a measure of the degree of compaction, we choose the change in the normalized volume, ΔV. The initial volume of a sample is $V = 1$ with $\Delta V = 0$; later, the volume decreases to $V = (1 - \Delta V)$ for an arbitrary compaction ΔV. In squeezing a sample it is assumed that only the pore fluid is taken out of the sample, decreasing its porosity. The compaction ΔV is closely related to the settlement, Δh, a term commonly used in soil mechanics, where a sediment of initial thickness h decreases

(settles) by Δh upon compaction, $\Delta V = \Delta h / h$ [e.g., *Hamilton*, 1959, p. 1424; *Tschebotarioff*, 1951, p. 105; *Tomlinson*, 1980, p. 135]. The compaction is related to the sediment porosity, ϕ, by

$$\phi = \frac{\phi_0 - \Delta V}{1 - \Delta V} \tag{1}$$

where ϕ_0 is the initial porosity (porosity of 80% enters the equation as 0.80). From the data of *Nobes et al.* [1986] we estimate the compaction in natural clay-rich sediments to be $\Delta V \approx 0.1$ at 50–100 m subbottom depth, $\Delta V \approx 0.3$ at 200–400 m depth and $\Delta V \approx 0.5$ for 500–1500 m depth. Therefore we are mainly interested in compaction values between 0 and 0.5. Changes in porosity with compaction from equation (1) are shown in Figure 1 for various initial porosities. We note that the relationship is quite smooth and close to linear for the lower compaction values.

Previously Published Models

Several models have been proposed to explain observed inclination shallowing, and we shall describe those relevant for this study. We refer to the models by the initials of their author(s). For the purpose of easy comparisons we have changed the symbols of some variables in the quoted references. The correct field inclination is denoted by I, and the observed inclination by $(I - \Delta I)$, where ΔI is the inclination shallowing.

Noncompacting Environment

For historical reasons we begin by describing two early models that predict inclination shallowing in noncompacting environments: first, the model by *King* [1955], which has influenced later models for compacting environments, and second, a model by *Griffiths et al.* [1960], which has been adapted for compaction in this study.

Model K. From redeposition studies of glacial sediments, *King* [1955] proposed a model to explain the observed inclination shallowing. He assumed two types of magnetic carriers: (1) a fraction f_K of platelike grains, magnetized parallel to their flat side, which would be lain down horizontally on contact at the sediment interface with zero inclination, and (2) a fraction $(1 - f_K)$ of spherical grains that accurately record the field inclination on average. By taking into account that initial dispersions affect the horizontal grains more, since there is a weaker aligning force ($\cos I$), he obtained the expression

$$\tan(I - \Delta I) = (1 - f_K) \tan I \tag{2}$$

[*King*, 1955, equation 5, p. 123]. His observations suggested that $f_K \approx 0.6$. This model has influenced several later models for inclination shallowing. *Nagata* [1962] criticized King for assuming the alignment to be proportional to the field strength, and he adjusted the equation to include strong alignment of individual grains, when the net moment is not proportional to the external field strength. However, we believe that King's argument is fully justified for geomagnetic field strengths, as will be discussed later.

Model GKRW. *Griffiths et al.* [1960] noted that sediment can usually not be clearly divided into well-contrasted groups of spherical and platelike particles, as required by model K. They were primarily interested in mechanisms at the sediment-water interface, which produce inclination shallowing. One of their models deals with rolling magnetized spheres into adjacent holes. The azimuth of the direction to the holes is random, but all the particles rotate about horizontal axes.

Consider first an example of four spheres, that prior to rotation, faithfully recorded the field direction, say, inclination I and declination zero. Now let these four particles rotate through an angle $\Delta\theta$, one toward north, one south, one east, and one west. For the northward and southward rotations, the declinations are unaffected and the changes of inclination will cancel. For the eastward and westward rotations the declination changes will cancel, but both the eastward and westward rotations will result in a shallowed inclination. The resultant direction of these four grains, after rotation, will preserve the declination but give shallow inclination.

Griffiths et al. [1960] solved this problem explicitly, starting with an ensemble where all the grains have initially an identical magnetic unit vector $\mathbf{m} = (\cos I, 0, \sin I)$. They obtained an exact expression for this vector after rotation through an angle $\Delta\theta$, about a horizontal axis with the azimuth λ. By integrating through all possible horizontal azimuthal directions λ, they found that the average magnetic vector after rotation is

$$\mathbf{m}_G = [(1/2)(1 + \cos\Delta\theta)\cos I, 0, \cos\Delta\theta \sin I] \tag{3}$$

The inclination shallowing can then be obtained by the exact expression

$$\tan(I - \Delta I) = \frac{2\cos\Delta\theta}{1 + \cos\Delta\theta} \tan I \tag{4}$$

[*Griffiths et al.*, 1960, equation 3, p. 377]. If we now define f_G as

$$f_G \equiv \frac{1 - \cos\Delta\theta}{1 + \cos\Delta\theta} \tag{5}$$

equation (4) becomes

$$\tan(I - \Delta I) = (1 - f_G) \tan I \tag{6}$$

which has the same form as equation (2) derived by *King* [1955] for a totally different model. The dependence of ΔI on $\Delta\theta$ for a fixed I, in equation (6) is shown in Figure 2*a*, and Figure 2*b* gives

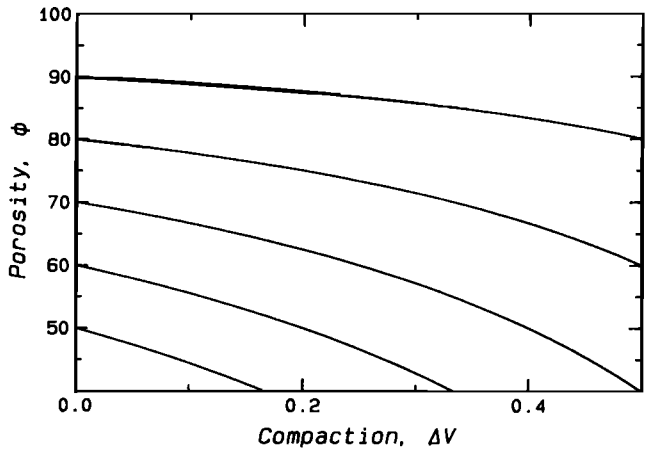

Fig. 1. Sediment porosity ϕ (%) as a function of compaction ΔV determined from equation (1) for initial porosities of $\phi_0 = 50, 60, 70, 80$, and 90%. For typical deep-sea sediment with porosities from 50 to 90% and compactions between 0 and 0.5 the relationship is very smooth and close to linear.

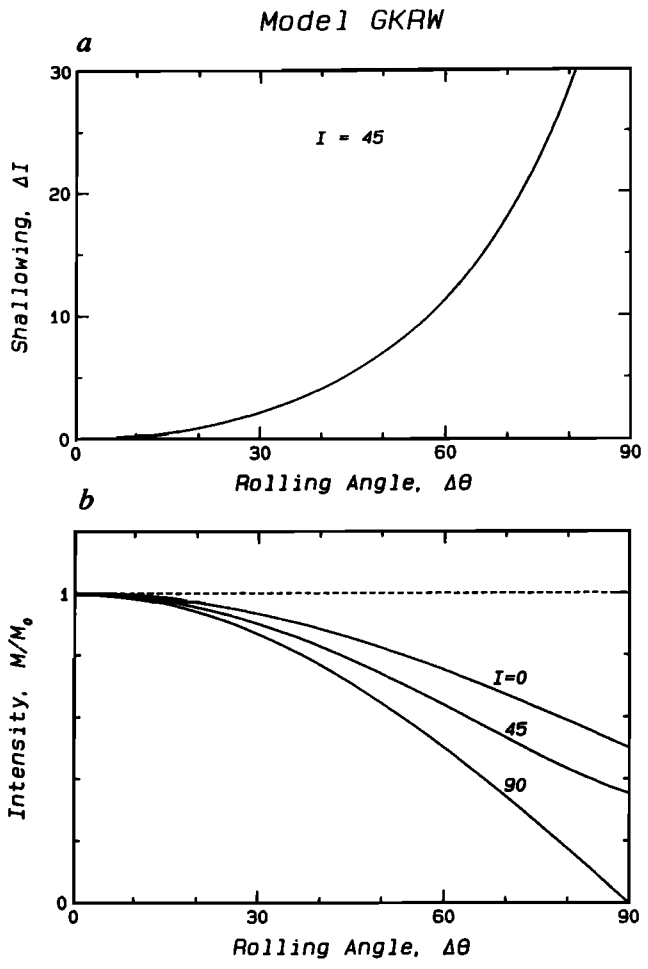

Fig. 2. Predictions of a model from *Griffiths et al.* [1960], here called model GKRW. (*a*) The inclination shallowing ΔI (deg) is shown as a function of the rolling angle $\Delta\theta$ (deg), for a fixed initial inclination of $I = 45°$, equation (6). Note that for small rolling angles, there is very little inclination shallowing; a rolling angle of 60° is needed to produce $\Delta I \approx 10°$. The nonlinearity of this function shows that for variable rolling angles the grains with very high rolling angles can outweigh those with lower values. (*b*) The intensity decrease, M/M_0, with rolling angle $\Delta\theta$ (deg) of model GKRW, from equation (52), for initial inclinations of $I = 0°$, 45°, and 90°.

the intensity deduced from equation (3) for various I. The rolling of magnetic spheres at the sediment water interface is analogous to the random rolling of grains due to rearrangement of sediment fabric in a compaction environment, which we explore further in this paper.

Compacting Environment

Blow and Hamilton [1978] proposed a compaction model which *Anson and Kodama* [1987] modified slightly to provide a better fit to their experimental data. The equations of these two models turn out to be very similar to the results of two of our rotating needle models, even though we start from totally different points of view.

Model BH. Blow and Hamilton [1978] proposed a compaction model, where the magnetization shallows in the same way as a passive line marker, which can be thought of as a sloping imagined soft line in the sediment, which shallows due to the shrinking vertical dimension. One way to view this model is to assume that the vertical axis of the remanence is reduced in the same proportion as the compaction of the vertical dimension of the sediment, with no alteration of the horizontal magnetization. Keeping in mind the form of the equation obtained by *King* [1955] for inclination shallowing (see model K), and using simple trigonometry, they deduced the mathematical expression

$$\tan(I - \Delta I) = (1 - \Delta V)\tan I \tag{7}$$

[*Blow and Hamilton*, 1978, Figure 6, p. 20]. However, the equation was not accompanied by a microscopic physical model, and their laboratory redepositional data were only marginally supportive of their model. *Ozima* [1980] conducted compaction experiments with ferromagnetic Co particles in a Cu matrix and found the inclination to follow the passive line marker upon deformation. Equation (7) of model BH is identical to equation (18) obtained for model 1b of this study.

Model AK. Anson and Kodama [1987] applied model BH to data from their laboratory compaction experiments with synthetic sediments. Their results suggested that model BH overestimates the inclination shallowing, and they modified equation (7) by a constant factor, a, such that

$$\tan(I - \Delta I) = (1 - a\,\Delta V)\tan I \tag{8}$$

[*Anson and Kodama*, 1987, equation 2, p. 685]. Best fits to the data were achieved for $a = 0.63 \pm 0.18$ for the acicular magnetite particles and $a = 0.54 \pm 0.18$ for the equidimensional magnetite. They proposed that the magnetite particles were electrostatically attached and rotated to the clay flake planes. Upon compaction the clay flakes would rearrange to more horizontal positions, resulting in inclination shallowing. Equation (8) turns out to be very similar to the equations of models 1c and 4a of this study (equations (22) and (72)).

Models of This Study

In this paper we propose several microscopic mechanisms to explain the compaction-induced inclination shallowing in sediments. The proposed models are used to derive mathematical expressions, relating inclination shallowing to sediment compaction. The proposed models can be categorized as (1) rotation of elongated or platy magnetic particles to more horizontal orientations, (2) rotation toward the horizontal of flat nonmagnetic fabric grains to which smaller magnetic grains are attached, (3) particle randomization leading to intensity decrease and possibly to inclination shallowing, and (4) the effects of expected initial within-sample dispersion.

Rotating Magnetic Needles

The simplest inclination shallowing models consider the rotation of elongated magnetic grains during sediment compaction. For simplicity we consider only very elongated needlelike grains magnetized along their long axis. We first assume perfect initial alignment of the needles with the external field, but later in this paper we examine the consequences of relaxing this constraint.

In the first least sophisticated model the needles are enclosed between two converging, rigid horizontal layers, the rigid matrix. In a second more realistic case we consider the surrounding sediment matrix as a soft compressible medium. The two fundamental assumptions in these first two models are that the magnetic grains are acicular and that the surrounding nonmagnetic sediment grains behave as a soft compressible medium around the rigid needles. Because the shapes of the magnetic particles in natural sediments probably range between needles and

equidimensional, these models predict an upper limit of inclination shallowing. Therefore we consider an additional model where a fraction of the remanence carriers rotates during compaction and the rest of the carriers are unaffected. The needle models are also applicable to magnetized flakes, if they are magnetized along the flake dip. For the surrounding sediment to approximate a soft medium with respect to the magnetic particles, one would expect that the nonmagnetic matrix grains are much smaller than the magnetic needles. Although observations show that fabric grains are often considerably larger than the magnetic grains, the matrix framework supported by organic binder might on average respond as a soft compressible medium, because of random and nondiscriminatory behavior, rotating some needles (flakes) more and some less than predicted. This random grain rotation will lead to an intensity decrease, which we consider later.

Model 1a : Rotating magnetic needles in rigid matrix. For this very simple model it is assumed that the remanence is carried by needle-shaped particles of length L, magnetized along their long axes. We assume that only compaction affects the remanence in the sediment. As compaction proceeds, the needles are not allowed to intrude the sediment above or below; only particle rotation is permitted. This mechanical model is shown in Figure 3*a*. From the left part of Figure 3*a* we find the trigonometric relation: $1 = L \sin I$, and from the right part we obtain $(1 - \Delta V) = L \sin (I - \Delta I)$. These can be connected through L to give

$$\sin (I - \Delta I) = (1 - \Delta V) \sin I \tag{9}$$

which relates the inclination shallowing to the compaction. The dependence of ΔI on I in equation (9) is shown in Figure 3*b*, for various ΔV and the dependence of ΔI on ΔV for a fixed initial inclination I in Figure 3*c*. For this model we note that the maximum effect of inclination shallowing is at very steep initial inclinations, but for lower initial inclinations the relationship between inclination shallowing and compaction is close to linear. For low initial inclinations this model predicts similar inclination shallowing as model BH.

The constraint of the model that the needles cannot penetrate the overlying and underlying sediment appears to be unrealistic, especially for very steep inclinations, but it may be more compatible for shallow initial inclinations. For very steep initial inclinations, we would expect the needles to intrude the oncoming sediment from above and below as the surrounding sediment is compacted, accompanied by relatively smaller grain rotation. This situation is considered in the next model.

Model 1b : Rotating magnetic needles in soft matrix. We now consider a single needle of length L, sloping at an angle I from the horizontal; see Figure 4*a*. We set the coordinate system such that the center of the needle is the origin which remains fixed through the compaction. From this perspective there is no translation of the needle but only rotation about a horizontal axis. The horizontal plane through the origin is called plane O. As seen from plane O, the sediment surrounding the needle will compact both from above and below. We restrict the surrounding sediment from moving horizontally, so in fact we can view this as a solid walled container depressed by a porous piston. We define r as the length along the needle from the origin; r is positive above the plane O and negative below; s is the vertical component of r: $s = r \sin I$. As the sediment compacts, by a small increment δV, the sediment at height s above the plane O will experience a movement toward the plane O: $s \rightarrow s - \delta s = s (1 - \delta V)$, leading to $\delta s = s\, \delta V$. The vertical force of the compacting sediment per unit length of the needle can be related to the displacement of the surrounding sediment by

$$F_v(r) = \alpha\, \delta s = \alpha r\, \delta V \sin I \tag{10}$$

where α is some constant, and the normal force on an element dr of the needle is

$$dF_n = F_v \cos I\, dr \tag{11}$$

which exerts a torque trying to rotate the needle toward shallower inclinations:

$$\tau = \int_{-L/2}^{L/2} r F_v(r) \cos I\, dr \tag{12}$$

with the solution

$$\tau = (\alpha L^3 / 24)\, \delta V \sin I \cos I \tag{13}$$

Now it is reasonable to expect that this torque will affect the rotation of the elongated particles, against the internal friction in the sediment. For a small compaction step, δV, the inclination shallowing, δI, is assumed to be proportional to the torque; $\delta I \sim \tau$, so

$$\delta I = \eta\, \delta V \sin I \cos I \tag{14}$$

where η is an efficiency parameter, indicating how effective the sediment is in rotating the needle. From equation (14) we can get the following differential equation:

$$\frac{dI}{dV} = \eta \sin I \cos I \tag{15}$$

and by definition we know that the inclination goes from I to $(I - \Delta I)$ as the volume goes from 1 to $(1 - \Delta V)$. Here we note that dV is not a linear measure of translation, so we transform dV to settlements dh, where $dV = dh / h$, and the thickness decreases from $h = 1$ to $h = (1 - \Delta V)$. We obtain

$$\int_I^{I-\Delta I} \frac{dI}{\eta \sin I \cos I} = \int_1^{1-\Delta V} \frac{dh}{h} \tag{16}$$

with the exact solution

$$\tan (I - \Delta I) = (1 - \Delta V)^{\eta} \tan I \tag{17}$$

One way to estimate the constant η is to assume that for very shallow initial inclinations ($I \approx 0°$), the inclination shallowing is predicted by model 1a (equation (9)), but then $\tan I \approx \sin I$, and $\tan (I - \Delta I) \approx \sin (I - \Delta I)$, and we therefore must have $(1 - \Delta V)^{\eta} \approx (1 - \Delta V)$, leading to $\eta = 1$, and the equation for model 1b

$$\tan (I - \Delta I) = (1 - \Delta V) \tan I \tag{18}$$

This equation is identical to equation (7) of model BH. The dependence of ΔI on I in equation (18) is shown in Figure 4*b*, for various ΔV, and the dependence of ΔI on ΔV for a fixed initial inclination I, in Figure 4*c*.

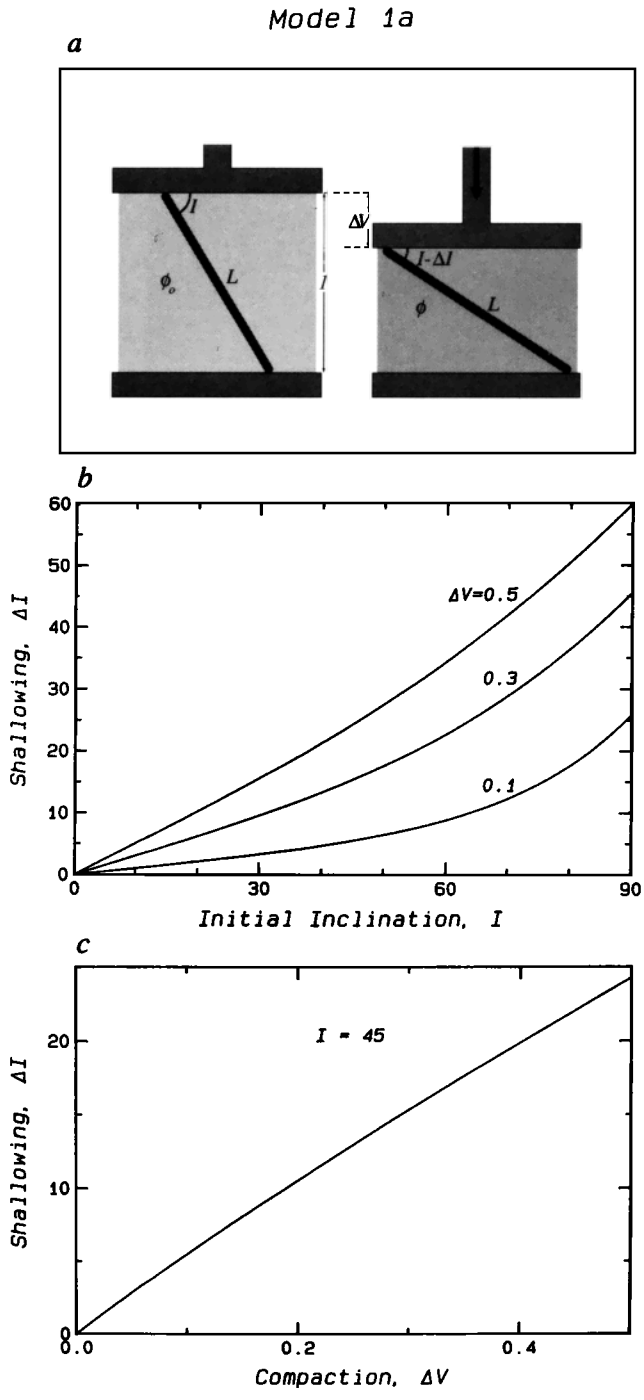

Fig. 3. Model 1a, rotating magnetic needles in rigid matrix, equation (9). (*a*) The magnetic needle of length L is enclosed between two rigid horizontal layers. Initially, on left the magnetic needle has the inclination I, and the sediment has the porosity ϕ_0. On right the layers have converged by ΔV and the water has been squeezed out so the porosity drops to ϕ and the inclination is shallower by ΔI. (*b*) The predicted inclination shallowing ΔI (deg) as a function of initial inclination I (deg), for different compactions $\Delta V = 0.1, 0.3, 0.5$. (*c*) The predicted inclination shallowing ΔI (deg) as a function of compaction ΔV, for initial inclination of $I = 45°$. The model predicts maximum ΔI at the magnetic poles ($I \approx \pm 90°$) but is thought to be unrealistic for steep inclinations.

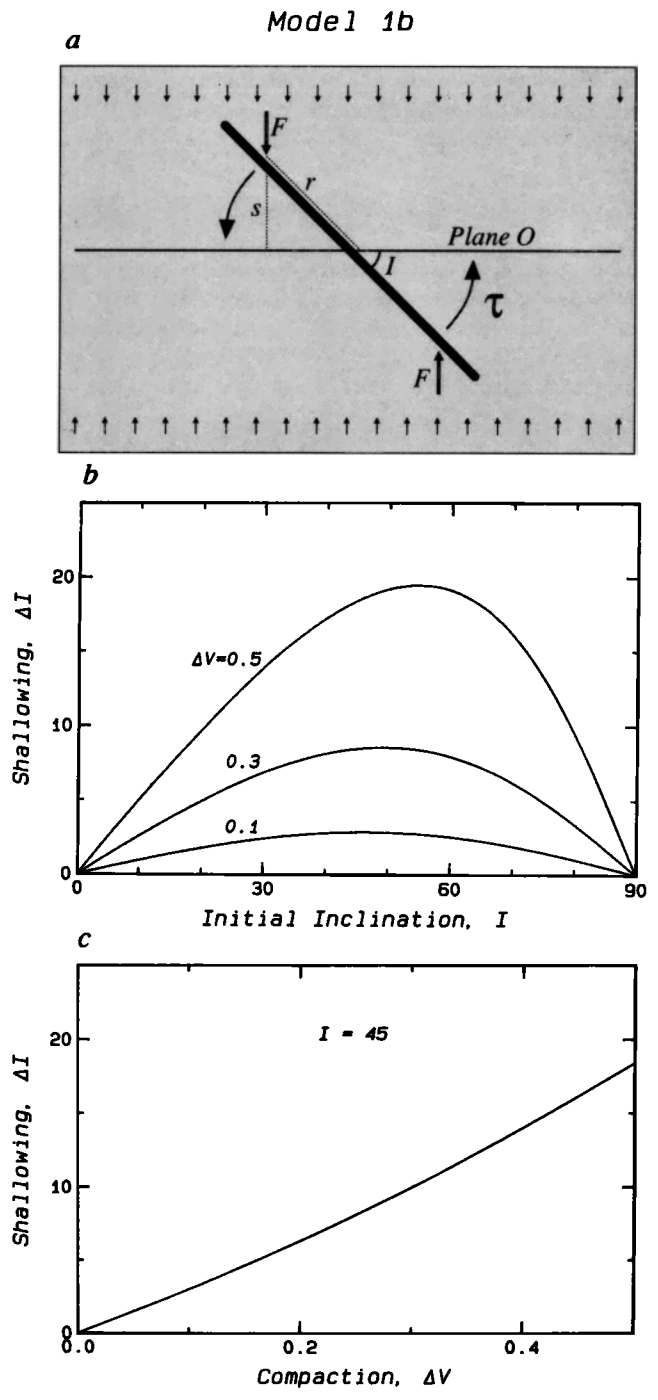

Fig. 4. Model 1b, rotating magnetic needles in soft matrix, equation (18). (*a*) The magnetic needle of length L is surrounded by soft material. As the material compacts, toward the plane O, it exerts torques on the needle, tending to rotate it to shallower inclinations. (*b*) The predicted inclination shallowing ΔI (deg) as a function of initial inclination I (deg), for different compactions $\Delta V = 0.1, 0.3, 0.5$. (*c*) The predicted inclination shallowing ΔI (deg) as a function of compaction ΔV, for initial inclination of $I = 45°$. For $I \approx \pm 90°$ the needle will not rotate but rather will intrude the oncoming sediment above and below.

For small compaction the maximum shallowing is predicted to be around initial inclinations of 45°, and the maximum moves toward slightly higher initial inclinations with increasing compaction. From equation (14) we see that for small compactions $\Delta I \approx \{180/\pi\}\ (1/2)\ \Delta V \sin 2I$ (the term $\{180/\pi\}$ gives ΔI in degrees), so for a fixed initial inclination I, the inclination shallowing ΔI is approximately linear with compaction ΔV, and that behavior extends over the compaction values of interest, as shown in Figure 4*c*.

Increased concentration of magnetic material. The previous two magnetic needle models (1a and 1b) do not account for random rotations of the magnetic grains, and during compaction the intensity increases with increasing concentration of magnetic particles per unit volume

$$M/M_0 = 1/(1-\Delta V) \tag{19}$$

In the absence of randomization, the needle models predict significant increases in intensity with compaction.

Model 1c : Two types of magnetic grain shapes in soft matrix. Magnetic particles in natural sediments have a range of shapes, and we therefore consider a mixture of magnetized grains; a fraction, f_n, are needles that obey the relation of model 1b (equation (18)) and the rest $(1-f_n)$ are equidimensional particles that do not rotate and preserve the initial inclination I during compaction. Upon compaction ΔV the inclination of the fraction f_n shallows by Δi

$$\tan(I-\Delta i) = (1-\Delta V)\tan I \tag{20}$$

The resultant vector is the sum of two vectors; one of length f_n dipping at $(I-\Delta i)$; the other of length $(1-f_n)$ dipping at I: $(f_n\cos(I-\Delta i), f_n\sin(I-\Delta i)) + ((1-f_n)\cos I, (1-f_n)\sin I)$, and we can find the total inclination shallowing from the total vector

$$\tan(I-\Delta I) = \frac{f_n\sin(I-\Delta i) + (1-f_n)\sin I}{f_n\cos(I-\Delta i) + (1-f_n)\cos I} \tag{21}$$

Using equation (20) and manipulating the trigonometric functions in equation (21), we obtain

$$\tan(I-\Delta I) = (1-cf_n\Delta V)\tan I \tag{22}$$

where the correction factor c is

$$c = 1/\left[f_n + (1-f_n)\sqrt{\cos^2 I + (1-\Delta V)^2\sin^2 I}\right] \tag{23}$$

Although c is weakly a function of f_n, ΔV, and I, it is practically equal to unity over values of interest. For $\Delta V = 0$, or $I = 0°$, $c = 1$, and for the range of compaction values ΔV from 0 to 0.5, initial inclinations I of 0° to 90°, and fractions f_n from 0 to 1, the correction factor c is always between 1 and 2. Indeed, if we further restrict our values to be $f_n > 0.5$, $I < 60°$, and $\Delta V < 0.3$, then c will be between 1.00 and 1.12.

We note that equation (22) is nearly identical to the formula used by *Anson and Kodama* [1987] (equation (8) of model AK in this paper), where we replace their arbitrary constant a by cf_n. The predictions of model 1c are compared to that of model AK in Figure 5. The dependence of ΔI on I in equations (8) and (22) is shown in Figure 5*a*, for various ΔV, and the dependence of ΔI on ΔV for a fixed initial inclination I is shown in Figure 5*b*. We note that the predictions are quite similar.

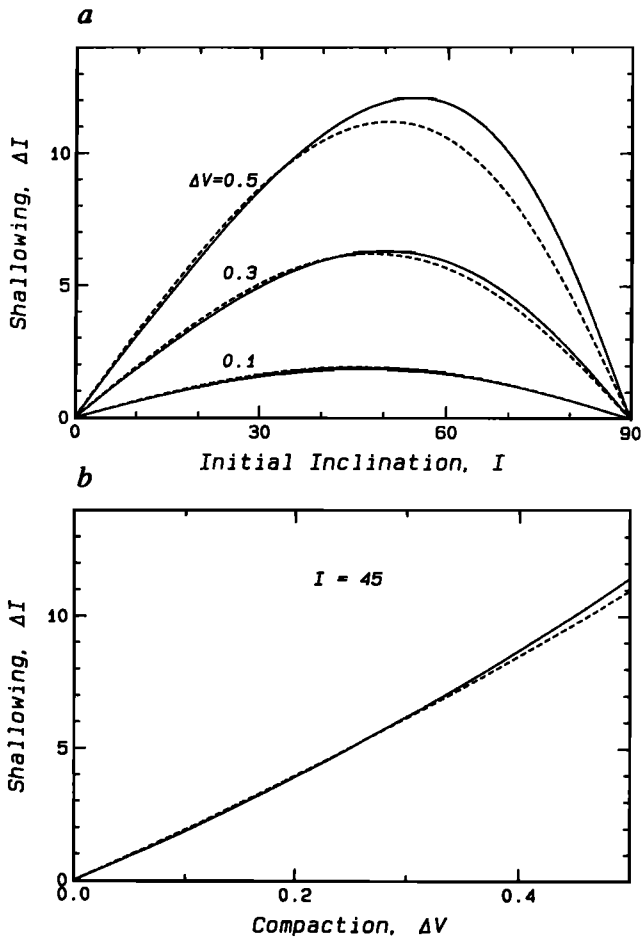

Fig. 5. Model 1c, two types of magnetic grain shapes in soft matrix, equation (22), where a fraction f_n of the magnetic carriers obey model 1b, and the rest $(1-f_n)$ are invariant upon compaction. Model 1c (solid lines) with $f_n = 0.62$, is compared to model AK (dashed lines), equation (8) with $a = 0.65$. (*a*) The inclination shallowing ΔI (deg) with initial inclination I (deg) for compactions $\Delta V = 0.1, 0.3, 0.5$. (*b*) The inclination shallowing ΔI (deg) with compaction ΔV for initial inclination of $I = 45°$. The two models show very similar results.

Collapsing Sediment Fabric

The most stable magnetic grains are expected to be small compared to the sediment fabric grains. If the magnetic grains are attached to fabric grains, they may rotate together during rearrangement of the matrix upon compaction. Clay flakes have strong shape anisotropy; however, any fabric with elongated or flat grains will give rise to a similar effect. In fact, any sediment, even composed of spherical grains, is subject to random grain rotations which may be predominantly about horizontal axes and will therefore give rise to the same effect. As the sediment compacts, the grains will rearrange themselves. Slight rearrangement of an individual grain can be described by a translation and rotation through an angle about some axis. The primary forces responsible for this rearrangement are the vertical forces of the gravitational compaction, and viscous drag due to the pore fluid flowing around grains mainly upwards to escape the decreasing pores. These forces will rotate the grains, predominantly about horizontal axes, analogous to model GKRW but now in compactional environments. This process will cause some randomization in the directions of the magnetic grains and also inclination shallowing.

In the following two collapsing fabric models we assume no relation between the orientations of flakes and magnetic grains. Similar to the needle models we assume perfect initial alignment of the magnetic moments with the external field, even though the fabric flakes may be oriented in a random fashion. Later in this paper we examine the consequences of allowing for initially dispersed magnetic moments. We assume now that the small magnetic carriers are somehow attached to the relatively large

fabric flakes in the sediment surface layers subsequent to the initial blocking of the remanence, and subsequently they rotate with the flakes during compaction. We define a normal vector perpendicular to the upper flat side of a flake. That normal deviates by the angle θ from the vertical, and θ is therefore also the dip of the flake plane from horizontal. The normal vector has the azimuthal direction λ from north. The normalized probability distribution of flakes with particular angle θ is $P_f(\theta)$, $0 \le \theta \le \pi/2$, $P_f(\theta)$ will change with compaction, as more of the flakes acquire shallower dips.

As the sediment compacts by ΔV, each flake with the initial dip θ will rotate through the angle $\Delta\theta$ to a shallower dip $(\theta - \Delta\theta)$. By analogy to model GKRW we see that these flakes will transform the initial magnetic unit vector (cos I, 0, sin I) to an equivalent of equation (3)

$$\mathbf{m}_G(\theta) = [(1/2)(1 + \cos\Delta\theta)\cos I, 0, \cos\Delta\theta \sin I] \quad (24)$$

We note that this is no longer a unit vector.

By connecting $\Delta\theta$ to a given ΔV and θ, we can find the resultant remanent magnetization after compaction by integrating equation (24) over all the fabric flakes

$$\mathbf{m}_f = \int_0^{\pi/2} \mathbf{m}_G(\theta) P_f(\theta)\, d\theta \quad (25)$$

By considering equation (24), we can split $\mathbf{m}_f$ in equation (25) into the three components (m_x, m_y, m_z):

$$m_x = \int_0^{\pi/2} (1/2)(1 + \cos\Delta\theta)\cos I\, P_f(\theta)\, d\theta \quad (26)$$

$$m_y = 0 \quad (27)$$

$$m_z = \int_0^{\pi/2} \cos\Delta\theta \sin I\, P_f(\theta)\, d\theta \quad (28)$$

Now we can calculate the magnetic inclination after the compaction through the relation $\tan(I - \Delta I) = m_z/m_x$:

$$\tan(I - \Delta I) = \frac{\sin I \int_0^{\pi/2} \cos\Delta\theta P_f(\theta)\, d\theta}{(1/2)\cos I \left[\int_0^{\pi/2} P_f(\theta)\, d\theta + \int_0^{\pi/2} \cos\Delta\theta P_f(\theta)\, d\theta\right]} \quad (29)$$

The probability distribution is assumed to be normalized, and by defining

$$F(\Delta V) = \int_0^{\pi/2} \cos\Delta\theta\ P_f(\theta)\ d\theta \quad (30)$$

we get

$$\tan(I - \Delta I) = \frac{2F(\Delta V)}{1 + F(\Delta V)} \tan I \quad (31)$$

Equation (31) can now be written on the same form as equation (2),

$$\tan(I - \Delta I) = (1 - f_f)\tan I \quad (32)$$

where

$$f_f \equiv \frac{1 - F(\Delta V)}{1 + F(\Delta V)} \quad (33)$$

So far we have avoided relating $\Delta\theta$ to θ and ΔV in equation (30), which in general is rather complex. However, two simple models can be set up. In the absence of other randomization one probably represents an overestimate and the other an underestimate of the flake rotation $\Delta\theta$. These models are intuitively similar to the rotating magnetic needle models, and are here called model 2a, collapsing rigid matrix, and model 2b, collapsing soft matrix.

Model 2a : Collapsing rigid matrix. A simplified flake-fabric model will give an overestimate of the rotation toward horizontal alignment in the absence of other randomization if we assume that each individual fabric flake is enclosed between two rigid horizontal surfaces through compaction. By analogy to model 1a (equation (9)), the rearrangement of the flakes is described by

$$\sin(\theta - \Delta\theta) = (1 - \Delta V)\sin\theta \quad (34)$$

See also Figure 3*a*. Through this equation we have connected $\Delta\theta$ to θ and ΔV. Furthermore, we assume that the flakes are initially spherically randomly distributed; hence

$$P_f(\theta)\, d\theta = \sin\theta\, d\theta \quad (35)$$

Now we can solve equation (30) by use of equations (34) and (35). The derivation is shown in the appendix, and the solution is found to be exactly

$$F(\Delta V) = 1 - \frac{(2\Delta V - \Delta V^2)^{3/2} - 3\Delta V^2 + 2\Delta V^3}{3 - 6\Delta V + 3\Delta V^2} \quad (36)$$

We use equation (33) to define a function f_a which can be approximated for ΔV between 0 and 0.5 as $f_a \approx 0.101\,\Delta V + 0.245\,\Delta V^2$. The equation for model 2a has the same form as equation (2)

$$\tan(I - \Delta I) = (1 - f_a)\tan I \quad (37)$$

The dependence of f_a on ΔV (from equations (33) and (36)) is shown in Figure 6*a*. The dependence of ΔI on I in equation (37) is shown in Figure 6*b*, for various ΔV, and the dependence of ΔI on ΔV for a fixed initial inclination I is shown in Figure 6*c*. The function f_a takes on much lower values than ΔV, leading to a very small inclination shallowing effect. Note that the function f_a is no longer linear with compaction, ΔV.

Model 2b : Collapsing soft matrix. As an underestimate of the flake rotation we use an analogy to model 1b (equation (18)), for the rotation of the fabric flakes. As before we assume that the initial dip θ diminishes to $(\theta - \Delta\theta)$ after a compaction ΔV.

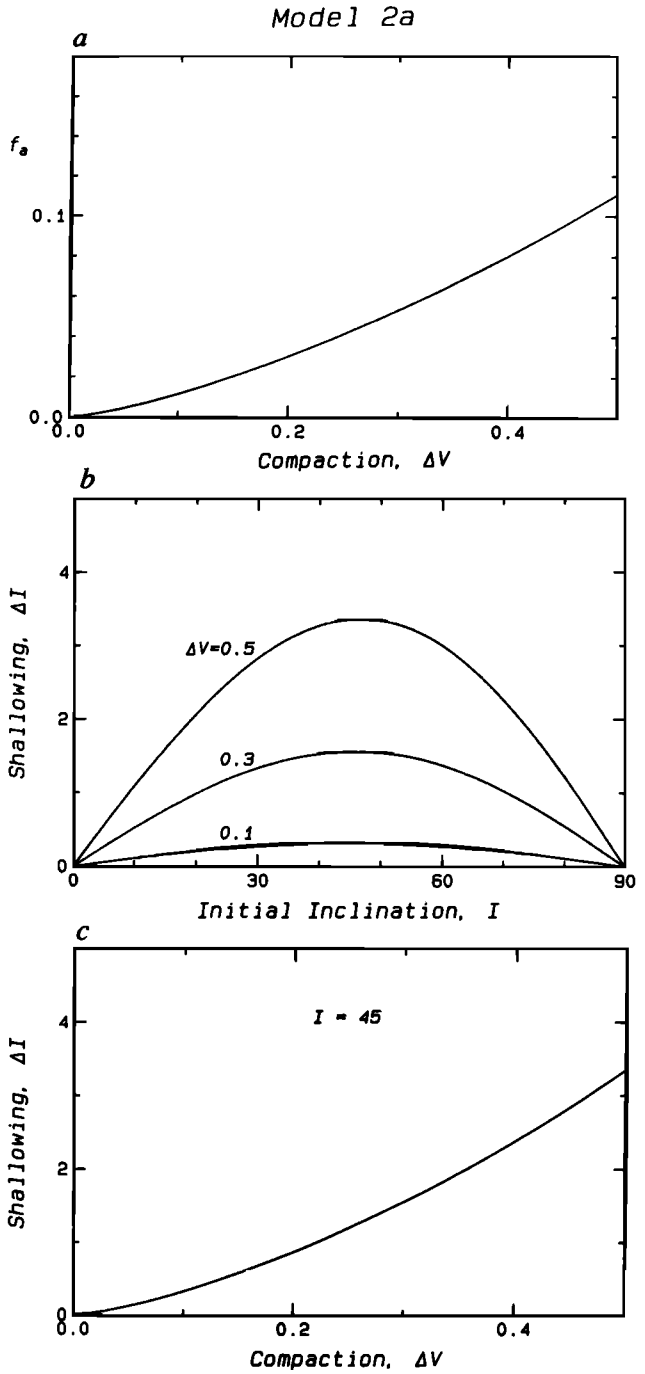

Fig. 6. Model 2a, collapsing rigid matrix, equation (37). This is thought to be an overestimate, when other randomization processes are omitted, of the inclination shallowing associated with rotation of the fabric grains to which smaller magnetic grains are attached. (*a*) The dependence of the function f_a on compaction ΔV, according to equations (33) and (36). (*b*) The predicted inclination shallowing ΔI (deg) as a function of initial inclination I (deg) for different compactions $\Delta V = 0.1, 0.3, 0.5$. (*c*) The predicted inclination shallowing ΔI (deg) as a function of compaction ΔV for initial inclination of $I = 45°$. There are strong similarities to models BH, AK, 1b, and 1c, but a factor of 3–10 in magnitude of the inclination shallowing.

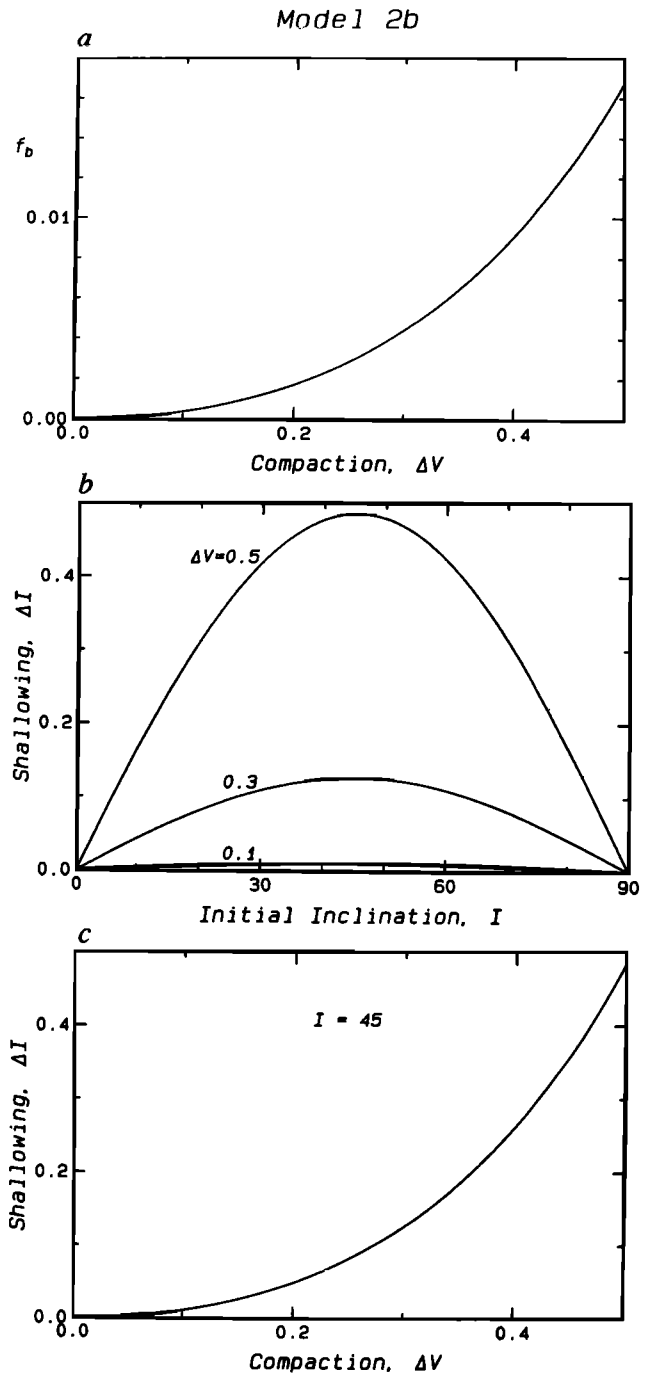

Fig. 7. Model 2b, collapsing soft matrix, equation (40). Note that all vertical scales differ by a factor of 10 from Figure 6. This is considered an underestimate of the inclination shallowing associated with the collapsing fabric. (*a*) The dependence of the function f_b on compaction ΔV, according to equations (33) and (39). (b) The predicted inclination shallowing ΔI (deg) as a function of initial inclination I (deg), for different compactions $\Delta V = 0.1, 0.3, 0.5$. (*c*) The predicted inclination shallowing ΔI (deg) as a function of compaction ΔV, for initial inclination of $I = 45°$. Note that this model predicts less than 0.5° inclination shallowing, which is hard to detect.

Therefore

$$\tan(\theta - \Delta\theta) = (1 - \Delta V)\tan\theta \tag{38}$$

Equation (30) is solved in the appendix, using equations (38) and (35). It is found to be exactly

$$F(\Delta V) = \frac{1}{2(2-\Delta V)} + \frac{(2-\Delta V)^2 - 1}{4(2-\Delta V)\sqrt{\Delta V(2-\Delta V)}} \ln\left(\frac{1+\sqrt{\Delta V(2-\Delta V)}}{1-\sqrt{\Delta V(2-\Delta V)}}\right) \tag{39}$$

As before, we define the function f_b using equation (33); f_b is shown in Figure 7*a* and can be approximated for low ΔV as $f_b \approx 0.0384\ \Delta V^2 + 0.1149\ \Delta V^4$. Therefore the equation for model 2b has the same form as equation (2):

$$\tan(I - \Delta I) = (1 - f_b)\tan I \tag{40}$$

The dependence of ΔI on I in equation (40) is shown in Figure 7*b*, for various ΔV, and the dependence of ΔI on ΔV for a fixed initial inclination I is shown in Figure 7*c*. This underestimate of the inclination shallowing in collapsing fabric is about a factor of 10 lower than by model 2a. For compaction values lower than 0.5 this model predicts a maximum inclination shallowing less than 0.5° which would be very difficult to detect in nature.

Magnetization intensities due to fabric rearrangement. With the rearrangement of fabric flakes in models 2a and 2b there is some dispersion of the magnetic moments and an associated intensity decrease. The concentration of magnetic material will increase as we sample more compacted sediment, as in model 3a. By connecting equation (33) to (30) and (26) – (28) we get the intensity

$$M/M_0 = \frac{\sqrt{1 - (2f_f - f_f^2)\sin^2 I}}{(1 - \Delta V)(1 + f_f)} \tag{41}$$

By inserting f_a for f_f in equation (41), we get the predicted intensity with compaction for model 2a, and by inserting f_b we get the prediction for model 2b. The intensity with compaction in model 2a is shown in Figure 8, for various initial inclinations I. We do not show the effect of model 2b, since the change is so small that it becomes indistinguishable from the bold reference curve, representing the increased concentration of magnetic material during compaction, equation (19). We note that even our overestimate (model 2a) does not decrease the intensity enough to account for the increased concentration effect. Therefore, in the absence of other randomization, the intensity will increase with compaction.

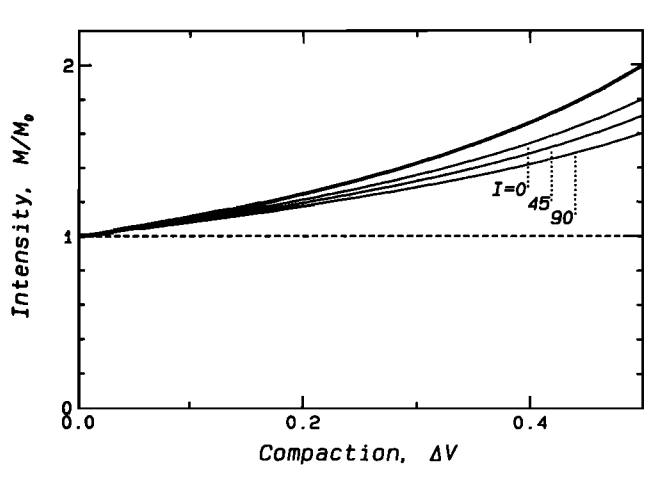

Fig. 8. Normalized intensity as a function of compaction for models 1 and 2. The bold curve represents the increased concentration of magnetic material, assuming no randomization, equation (19). The higher intensities are caused by more magnetic material per unit volume. Also shown is the intensity predicted by model 2a, collapsing rigid matrix (the three plain curves), equation (41), for initial inclinations $I = 0°$, 45°, and 90°. The effect of model 2b (not shown in the figure) is so minute that the intensities become indistinguishable from the bold reference curve. The two collapsing fabric models (2a and 2b) do not predict enough dispersion of the magnetic moments to account for the increased concentration of magnetic material due to the compaction.

Microscopic Kneading of the Sediment

The previous models are deterministic descriptions of inclination and intensity changes with compaction. Decrease of the intensity of magnetizations have been observed during compaction, both with depth (or time) in sediment cores and compaction in laboratory experiments. This effect has been attributed to randomization or misalignment of the magnetic grains [*Stober and Thompson*, 1979; *Karlin and Levi*, 1982]. As seen in Figure 8 it is impossible to decrease the intensity with the models 1a, 1b, 2a, and 2b, so we consider two models of random grain rotations. Model 3a, unbiased randomization of grains, will not affect the inclination but will decrease the intensity, and model 3b, random rolling of grains about horizontal axes, will decrease the intensity and also will introduce inclination shallowing through the rolling spheres effect described by *Griffiths et al.* [1960] (model GKRW). The magnetic torques of the grains are negligible compared to the mechanical forces responsible for their rearrangements, so for these two models we assume that growth of secondary remanence during grain randomization [*Tucker*, 1980] can be neglected.

Model 3a : Unbiased randomization of grains. A simple way of looking at an unbiased randomization process is to assume a group of initially parallel magnetic moments, which will be rotated through some angles, θ. Some grains will experience small rotations, and others greater. It is reasonable to assume that these angular deviations can be described by the Fisher distribution P_F, which is analogous to the normal distribution on a sphere [*Fisher*, 1953]

$$P_F(\theta)\,d\theta = \frac{\kappa}{2\sinh\kappa} e^{\kappa\cos\theta}\sin\theta\,d\theta \tag{42}$$

where κ is the precision parameter of the distribution. Due to the symmetry of the random rotations we expect that the average magnetic direction of the sample will not change. The magnetic intensity of a unit vector, that has rotated through θ, will therefore only add cos θ to the total intensity, which can then be calculated by

$$M/M_0 = \int_0^{\pi} P_F(\theta)\cos\theta\,d\theta \tag{43}$$

To solve equation (43), it is convenient to make the substitution $s \equiv \cos\theta$, which transforms it to

$$M/M_0 = \frac{\kappa}{2\sinh\kappa} \int_{-1}^{1} s\,e^{\kappa s}\,ds \tag{44}$$

with the solution

$$M/M_0 = \coth\kappa - 1/\kappa \tag{45}$$

which is the Langevin function $L(\kappa)$. Convenient approximations to the Langevin function ($L(\kappa) \approx \kappa/3$ for low κ, and $L(\kappa) \approx 1 - 1/\kappa$ for high κ) are not fully applicable since we are also interested in intermediate values. We can also take into account the increased concentration effect due to an arbitrary compaction ΔV, even though we are not relating κ to ΔV

$$M/M_0 = \frac{\coth \kappa - 1/\kappa}{1 - \Delta V} \quad (46)$$

where κ can, for instance, be related to θ_{63}, the angular standard deviation, that is, 63% of the moments are rotated through an angle less than θ_{63}

$$\cos \theta_{63} = 1 + (1/\kappa) \ln [\, 1 - 0.63\, (\, 1 - e^{-2\kappa}) \,] \quad (47)$$

The normalized intensity in equation (46) is shown as a function of θ_{63} in Figure 9*a* for various ΔV.

So far in this model we have assumed no initial within-sample dispersion. To address the problem of initial dispersion, we consider a partially randomized sample where different subsets of grains have parallel magnetic moments. The total magnetization of the ith subset is m_i, and the magnetization direction of the ith subset is at angle θ_i to the average direction of the whole sample, and it contributes $m_i \cos \theta_i$ to the sample's total intensity. Upon randomization the subset under consideration retains its average direction, due to symmetry, but there is a decrease in intensity $m_i L(\kappa)$ (as described by equation (45)), because all the moments of the subset were initially parallel. Since neither the subset's direction nor the direction of the whole sample have changed during randomization, our subset will contribute $m_i L(\kappa) \cos \theta_i$ to the total intensity. The intensity contributions of all subsets will decrease as $L(\kappa)$, and the total moment will therefore also decrease as $L(\kappa)$. Therefore randomization in samples with initial dispersion also obeys equation (45).

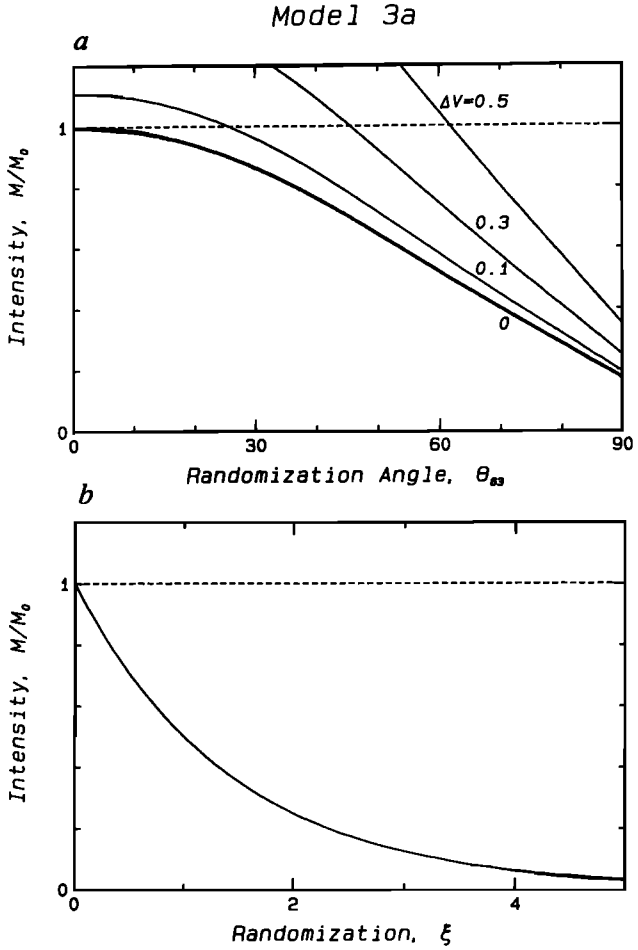

Fig. 9. Model 3a, unbiased randomization of grains, equation (46). (*a*) Normalized intensity predicted as a function of the characteristic rotation angle θ_{63} (angular standard deviation), equation (47), for different compaction values $\Delta V = 0$ (bold curve), and 0.1, 0.3, 0.5. Here we are only considering how much randomized grain rotation is needed to depress the intensity. Note that a considerable grain rotations are needed to offset the intensity of magnetization. (*b*) Normalized intensity versus the randomization parameter ξ, equation (49). The term randomization is introduced as a fundamental property of the net magnetic moment of a sedimentary sample. Randomizations are independent of distribution of magnetic moments and other initial properties of a given sediment. Randomizations are additive.

From this result we see that a sample undergoing randomization by κ_1 will have intensity $M_1/M_0 = L(\kappa_1)$. If we take this randomized sample and randomize it again by arbitrary chosen κ_2, its intensity will be $M_2/M_0 = L(\kappa_1)\, L(\kappa_2)$ and so on. We now define the term randomization, ξ,

$$\xi \equiv - \ln [\, L(\kappa) \,] / \ln 2 \quad (48)$$

The factor (1/ln 2) gives ξ the property that by increasing the randomization by 1 will decrease the intensity by a factor of 2. With the aid of equation (45) we see

$$M = M_0\, e^{-\xi \ln 2} \quad (49)$$

and for a randomization ξ_1 followed by ξ_2, followed by ξ_3 and so on, we see that the total randomization is partially additive

$$\xi_{\text{total}} = \xi_1 + \xi_2 + \xi_3 + \cdots \quad (50)$$

This additivity of randomization is valid for all κ values, $0 \le \kappa \le \infty$. In Figure 9*b* we show how the intensity decreases with randomization. For high κ, $L(\kappa) \approx 1 - 1/\kappa$, and $\ln (1 - \varepsilon) \approx -\varepsilon$; therefore, from equation (48) we get $\xi \sim 2/\kappa$ for high κ values. This is the variance of the Fisher distribution. However, for low κ, neither $2/\kappa$ nor the variance are partially additive as is the randomization.

From equation (49) we note that for a sedimentary section with constant reworking per unit depth (or even unit of time) we can define $\zeta \equiv \ln 2\, \xi/h$ (where h is the thickness of the section) and we would expect an intensity profile with depth z

$$M(z) = M_0\, e^{-\zeta z} \quad (51)$$

where M_0 would now represent intensity at the top ($z = 0$). We therefore predict exponential decrease of intensities in sediments where the randomization is constant per unit depth.

This model predicts no directional changes but leads to the next model where we consider what happens if the randomization is limited to rotations about horizontal axes.

Model 3b : Random rolling of grains about horizontal axes. Instead of trying to relate $\Delta\theta$ to θ and ΔV in the collapsing fabric models (2a and 2b), we can consider what effect a grain rotation about horizontal axes would have on the intensity of the remanent magnetization, independent of how much compaction it would require. For a rotation of the magnetic grains about randomly distributed horizontal axes, by some fixed characteristic angle $\Delta\theta$, we get the inclination shallowing shown in equation (6). From equation (3) (in model GKRW) one easily obtains the intensity decrease as

$$M/M_0 = \sqrt{(1/4)\, (1 + \cos \Delta\theta)^2 \cos^2 I + \cos^2 \Delta\theta \sin^2 I} \quad (52)$$

Note that we do not relate $\Delta\theta$ to ΔV in this model. The effect of equation (52) is shown in Figure 2*b* for various initial inclinations.

Model GKRW shows the inclination shallowing when all grains roll by the same rolling angle $\Delta\theta$. Furthermore, we have connected rolling of grains to compaction in models 2a and 2b in a particular deterministic way. In reality, one would expect some grains to roll more and others less, depending on many unpredictable factors. Therefore an obvious extension of model GKRW is to allow for a distribution in $\Delta\theta$, where rolling occurs about horizontal axes. Distribution of rotation angles about a fixed axis can be described as a distribution on a circle. The "normal" distribution on a circle is the Von Mises distribution, closely related to the Fisher distribution on a sphere [*Von Mises*, 1918; *Fisher*, 1953; *Mardia*, 1972, p. 57]

$$P_M(\Delta\theta)\, d(\Delta\theta) = \frac{1}{2\pi I_0(\kappa)} e^{\kappa\cos\Delta\theta}\, d(\Delta\theta) \tag{53}$$

where $I_0(\kappa)$, the hyperbolic Bessel function of order zero (sometimes also called the modified Bessel function), is used to normalize the distribution. $I_0(\kappa)$ can not be written in terms of elementary functions. In choosing the Von Mises distribution to describe the rolling angles, we do not take into account that some grains are elongated and will resist rolling through the horizontal. However, in the absence of detailed knowledge of individual grain behavior, we take the Von Mises distribution with zero mean (symmetric rolling) as a good first-order estimate. The Von Mises distribution is shown in Figure 10*a*, for selected values of κ.

Now we use the result of *Griffiths et al.* [1960], ($\mathbf{m}_G$ in equation (3) in this paper) to determine how the unit vector $\mathbf{m} = (\cos I, 0, \sin I)$ rotates to $\mathbf{m}_H$

$$\mathbf{m}_H = \int_{-\pi}^{\pi} P_M(\Delta\theta)\, \mathbf{m}_G(\Delta\theta)\, d(\Delta\theta) \tag{54}$$

or split into the components (m_{Hx}, m_{Hy}, m_{Hz})

$$m_{Hx} = \int_{-\pi}^{\pi} \frac{1}{2\pi I_0(\kappa)} e^{\kappa\cos\Delta\theta}(1/2)(1+\cos\Delta\theta)\cos I\, d(\Delta\theta) \tag{55}$$

$$m_{Hy} = 0 \tag{56}$$

$$m_{Hz} = \int_{-\pi}^{\pi} \frac{1}{2\pi I_0(\kappa)} e^{\kappa\cos\Delta\theta}\cos\Delta\theta\sin I\, d(\Delta\theta) \tag{57}$$

with the solutions

$$m_{Hx} = (1/2)\,[\,1 + I_1(\kappa)/I_0(\kappa)\,]\cos I \tag{58}$$

$$m_{Hz} = [\,I_1(\kappa)/I_0(\kappa)\,]\sin I \tag{59}$$

where $I_1(\kappa)$ is the hyperbolic Bessel function of first order.

Now we can calculate the inclination shallowing

$$\tan(I-\Delta I) = \frac{2\, I_1(\kappa)/I_0(\kappa)}{1 + I_1(\kappa)/I_0(\kappa)}\tan I \tag{60}$$

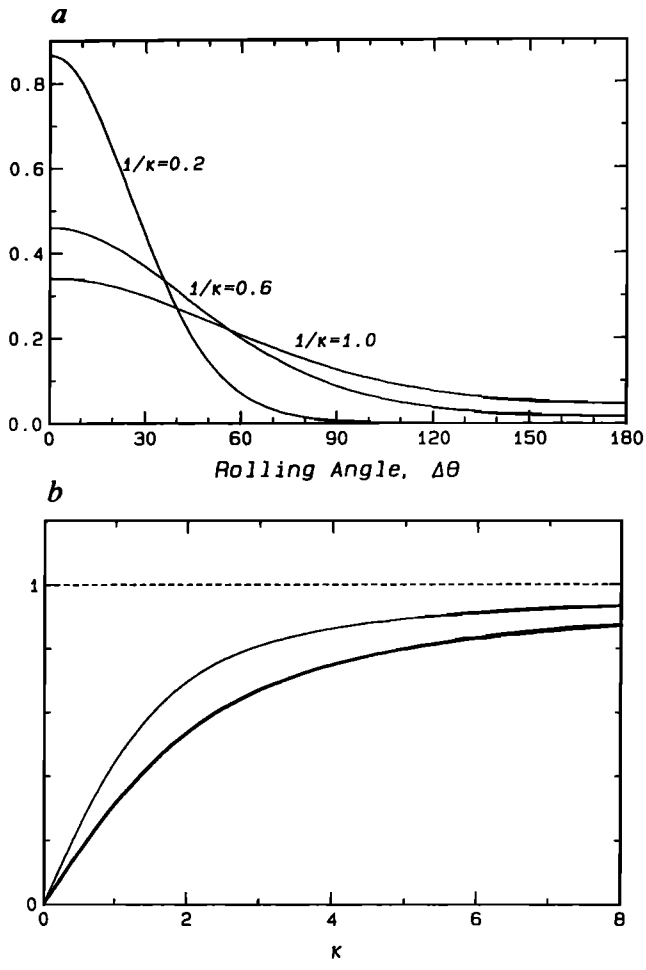

Fig. 10. Fundamental functions used in models 3a and 3b. (*a*) The Von Mises distribution, equation (53), is shown versus the rolling angle $\Delta\theta$ (deg), for spread parameters of $1/\kappa = 0.2, 0.6, 1.0$. We note that these spread values call for considerable grain rolling. (*b*) The Langevin function $L(\kappa)$ (solid), equations (45) and (65), compared to the ratio of the hyperbolic Bessel functions $I_1(\kappa)/I_0(\kappa)$ (dashed), that appears in equations (58) through (63). These functions are very similar. For low κ ($\kappa < 0.5$) they can be approximated as $L(\kappa) \approx \kappa/3$, and $I_1(\kappa)/I_0(\kappa) \approx \kappa/2$, and for high κ ($\kappa > 3$) they can be approximated as $L(\kappa) \approx 1 - 1/\kappa$, and $I_1(\kappa)/I_0(\kappa) \approx 1 - 1/(2\kappa)$.

and by defining

$$f_h \equiv \frac{1 - I_1(\kappa)/I_0(\kappa)}{1 + I_1(\kappa)/I_0(\kappa)} \tag{61}$$

we get the common form

$$\tan(I-\Delta I) = (1-f_h)\tan I \tag{62}$$

The intensity is

$$M/M_0 = \sqrt{(1/4)\,[1 + I_1(\kappa)/I_0(\kappa)]^2\cos^2 I + [I_1(\kappa)/I_0(\kappa)]^2\sin^2 I} \tag{63}$$

We note that the hyperbolic Bessel functions always occur as the ratio $I_1(\kappa)/I_0(\kappa)$, and even though both $I_0(\kappa)$ and $I_1(\kappa)$ blow up very fast with increasing κ, their ratio is very similar to the Langevin function. For high κ, $I_1(\kappa)/I_0(\kappa) \approx 1 - 1/(2\kappa) \approx L(2\kappa)$, and for low κ, $I_1(\kappa)/I_0(\kappa) \approx \kappa/2 \approx L(1.5\kappa)$. The Langevin function

and the ratio of the hyperbolic Bessel functions is shown in Figure 10*b*. The characteristics of model 3b are shown in Figure 11, where we show the exact solutions of equations (62) and (63), using the inverse of the precision parameter, which we call the "spread" parameter ($1/\kappa$), as a measure of random rolling. We note that random rolling about horizontal axes, leading to intensity decreases of 20–50%, results in significant inclination shallowing.

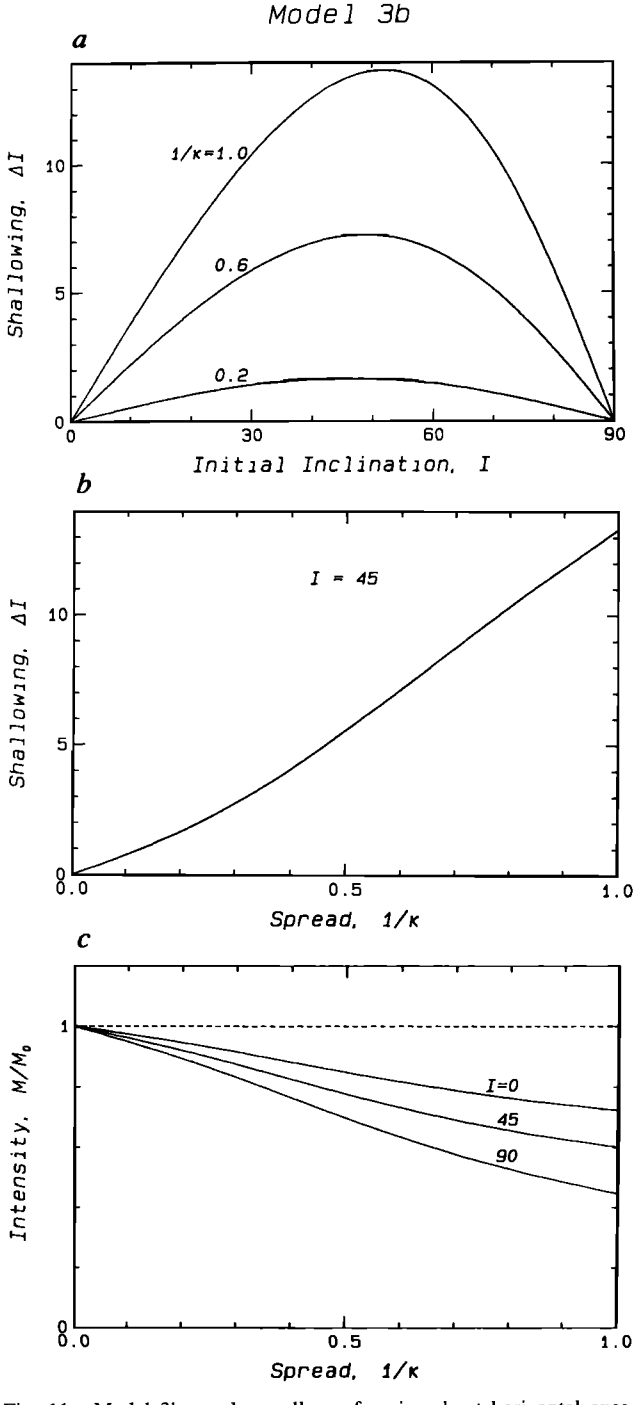

Fig. 11. Model 3b, random rolling of grains about horizontal axes, equation (62). (*a*) The inclination shallowing ΔI (deg) versus initial inclination I (deg), for fixed amounts of random rolling of sediment grains about horizontal axes, measured by the "spread" parameter $1/\kappa = 0.2, 0.6, 1.0$. (*b*) The inclination shallowing ΔI (deg) versus spread parameter $1/\kappa$, for a fixed initial inclination $I = 45°$. (*c*) The normalized intensity changes with the spread parameter $1/\kappa$, for initial inclinations $I = 0°, 45°$, and 90°. In essence we have transformed a model by *Griffiths et al.* [1960], model GKRW in this paper, to allow for a distribution in rolling angle, resulting in significant inclination shallowing.

We believe that microscopic randomization of sediment is an important mechanical factor in sediments. The random rolling about horizontal axes may be much less important than the isotropic randomization but still sufficiently significant for producing inclination shallowing. Different lithologies and physical properties may control the amount of isotropic randomization relative to random rolling about horizontal axes, making it difficult to predict the magnitude of this effect. However, the ratio between these two processes may be unique for a given lithology and once established, prediction is possible.

Initial Dispersion of the Magnetic Moments

Initial distribution. We are interested in the initial within-sample distribution of magnetic moments. *King* [1955] assumed relatively low degree of alignment of magnetic moments within the sediment, so that the intensity of magnetization would be proportional to the external field strength. *Nagata* [1962] was first to study distributions of within-sample dispersions. To study the probable initial distribution of magnetic moments, we consider the acquisition of remanence in the sediment close to the sediment water interface. A magnetic particle of net moment m oriented at an angle θ to the external magnetic field H will have a torque, $m H \sin \theta$, which will tend to rotate the grain toward the field direction, while thermal agitations due to Brownian motions compete with this aligning force [*Collinson*, 1965]. This problem is identical to Langevin's classical theory of paramagnetism of the alignment of molecules with magnetic moments in an external magnetic field [*Langevin*, 1905; *Chikazumi*, 1964, pp. 60-62]. In fact, any randomization agent, such as bioturbation, will fight the alignment. The distribution of the magnetic moments in Langevin's theory is

$$P(\theta)\, d\theta = \frac{N\ (m H / k T)}{2 \sinh\ (m H / k T)}\, e^{(m H / k T) \cos \theta} \sin \theta\, d\theta \qquad (64)$$

where k is Boltzmann's constant, T the absolute temperature, and N is the number of individual moments (Nm is the total moment, when all moments are parallel). We note that if we normalize this distribution to unity ($N = 1$), this is the Fisher distribution with $\kappa = m H / k T$. *Langevin* [1905] found the net moment to be

$$M/M_0 = \coth \kappa - 1/\kappa \qquad (65)$$

since then called the Langevin function $L(\kappa)$. Even though it has been shown that the distribution and the net moment may vary with grain size [*Stacey*, 1972], we consider equations (64) and (65) as an adequate first-order estimate of the initial within-sample distribution of the magnetic moments and its net moment.

It should be possible to estimate the amount of initial dispersion in sediments. *Kent* [1973] obtained a linear dependence of the remanence on the external field for redeposited deep-sea sediments in fields up to 120 μT. This implies that the external fields were still in the linear range of the Langevin function, indicating that M/M_0 is less than 10% and $\kappa < 0.3$. Similarly, *Khramov* [1968] observed linear behavior to fields 10 times the present value, leading to the estimate $M/M_0 < 3\%$ and $\kappa < 0.1$. These estimates provide an upper limit to the alignment, but they indicate relatively poor alignment.

In laboratory depositional experiments with synthetic sediment one has better control of the concentration and domain state of the magnetic material, which might lead to better estimates of M/M_0. Our best estimate of probable values of M/M_0 comes from the data

of *Anson and Kodama* [1987]. From their description we estimate that each of their samples contain approximately 10^{-5} kg of magnetite. Their acicular magnetite (0.45 μm × 0.07 μm) is clearly single domain [e.g., *Levi and Merrill*, 1978], for which we can assign the saturation magnetization of magnetite 92 A m^2 kg^{-1}. Therefore, if all the magnetite needles in a sample (10^{-5} kg) were aligned parallel, the sample would have the magnetic moment 10^{-3} A m^2. The magnetic moments of their samples average to 15.5×10^{-7} A m^2 ranging from 4.1 to 36.3 at the lowest compaction values of the 14 samples [*Anson and Kodama*, 1987, Table 1]. Therefore we can estimate the alignment for these samples: $M/M_0 \approx 0.2\%$, and $\kappa \approx 0.005$. By taking into account possible impurities, crystal imperfections, and probable grain size distribution of their magnetite we note that this will be a slight underestimate of alignment, but accounting for such factors can probably not bring the estimate of the alignment above 1%. We conclude that the orientation of submicron magnetic grains is probably nearly random in natural sediments, redeposited natural sediments, and synthetic sediments. Of course, there is a small but sufficient orientation bias toward the ambient field direction to account for the net observed remanent magnetism.

Model 4a : Initial within-sample dispersion. So far we have ignored any effects of initial within-sample dispersion of magnetic moments on the inclination shallowing. Within-sample dispersion would tend to smear out the dependence of ΔI on I. By assuming that individual grains obey an equation of the form

$$\tan (i - \Delta i) = (1 - \varepsilon) \tan i \tag{66}$$

we see that Δi at middle inclinations (about 45°) will be less than predicted by equation (66) due to smearing. From symmetry of the expected dispersion we note that the inclination shallowing, Δi, will still be zero at $I = 0°$ and $\pm 90°$.

We solve the problem of initial dispersion by starting with a unit vector composed of inclination, i, and declination, d:

$$\mathbf{m} = (\cos i \cos d , \cos i \sin d , \sin i) \tag{67}$$

This vector makes the angle θ with the sample's mean direction (inclination I and declination of zero) which can be calculated from the scalar product of $\mathbf{m}$ and (cos I, 0, sin I)

$$\cos \theta = \sin I \sin i + \cos I \cos i \cos d \tag{68}$$

The unit vector, $\mathbf{m}$, is subsequently rotated to a new shallower inclination ($i - \Delta i$), defined by equation (66), but the declination is kept unaltered at d. The unit vector $\mathbf{m}$ is therefore transformed to

$$\mathbf{m}' = [\cos (i - \Delta i) \cos d , \cos (i - \Delta i) \sin d , \sin (i - \Delta i)] \tag{69}$$

The vectors $\mathbf{m}$ are assumed to obey the Fisher distribution about the mean direction; hence the frequency density of the vector $\mathbf{m}$ is proportional to

$$e^{\kappa \cos \theta} \tag{70}$$

To get the total inclination shallowing, we therefore integrate over all directions (d,i), weighted by equation (70) and a geometrical factor of cos i:

$$\tan (I - \Delta I) = \frac{m_{z\text{-average}}}{m_{x\text{-average}}}$$

$$= \frac{\displaystyle\int_{-\pi/2}^{\pi/2} \int_0^{2\pi} \cos i \; e^{\kappa \cos \theta} \sin (i - \Delta i) \; dd \, di}{\displaystyle\int_{-\pi/2}^{\pi/2} \int_0^{2\pi} \cos i \; e^{\kappa \cos \theta} \cos (i - \Delta i) \cos d \; dd \, di} \tag{71}$$

where ($i - \Delta i$) and θ are functions of I, i, d, and ε through equations (66) and (68). To solve this analytically turns out to be complicated; instead we make the approximation

$$e^{\kappa \cos \theta} \approx 1 + \kappa \cos \theta \tag{72}$$

which is reasonable for small κ. With this approximation, equation (71) is solved in the appendix and has the solution

$$\tan (I - \Delta I) = (1 - b \, \varepsilon) \tan I \tag{73}$$

where

$$(1 - b \, \varepsilon) =$$

$$= \frac{2 (1-\varepsilon) \arccos(1-4\varepsilon+2\varepsilon^2) - 4 (1-\varepsilon)^2 \sqrt{2\varepsilon-\varepsilon^2}}{-(1-4\varepsilon+2\varepsilon^2) \arccos(1-4\varepsilon+2\varepsilon^2) + 2 (1-\varepsilon) \sqrt{2\varepsilon-\varepsilon^2}} \tag{74}$$

Exact solution to equation (71) may be written on the form of equation (73), where b would be a function of ε and also slightly dependent on κ and I. However, with the approximation in equation (72), b becomes independent of κ and I. We have studied numerical solutions to the exact form of equation (71) and found the solution to start deviating from the approximation in equations (73) and (74) when $\kappa > 0.5$ (1% error in b). Furthermore, if the initial distribution were not exactly Fisherian, this would affect the function b. Therefore we believe the approximation in equation (72) to be adequate. For ε between 0 and 0.5 we can estimate b in equation (74) as

$$b \approx 0.593 + 0.232\varepsilon \tag{75}$$

The choice between equations (74) and (75) depends on the need for accuracy. The results of this model are shown in Figure 12. We note that a sediment obeying the equation of model BH on a microscopic level but composed of rather dispersed moments will appear to be obeying model AK macroscopically with the numerical value $a \approx 0.65$, within error bounds of the estimate of a that *Anson and Kodama* [1987] obtained experimentally. We therefore compare the predicted inclination shallowing of model AK with $a = 0.65$, model 1c with $f_n = 0.62$, and model 4a with $\varepsilon = \Delta V$, in Figure 13*a*. They are very similar.

For the above estimate of b, we have assumed that the sediment obeys equation (66) on microscopic level. All our models are of this form, except model 1a. In the appendix we show that assuming equation (9) (model 1a) on a microscopic level results macroscopically in the same form as equation (73) but with a different constant b, which we call b'. In the appendix we show that b' is

$$(1 - b' \varepsilon) = \frac{2 (1-\varepsilon)^3}{((1-\varepsilon)^2-1) \, \boldsymbol{K}(1-\varepsilon) + ((1-\varepsilon)^2+1) \, \boldsymbol{E}(1-\varepsilon)} \tag{76}$$

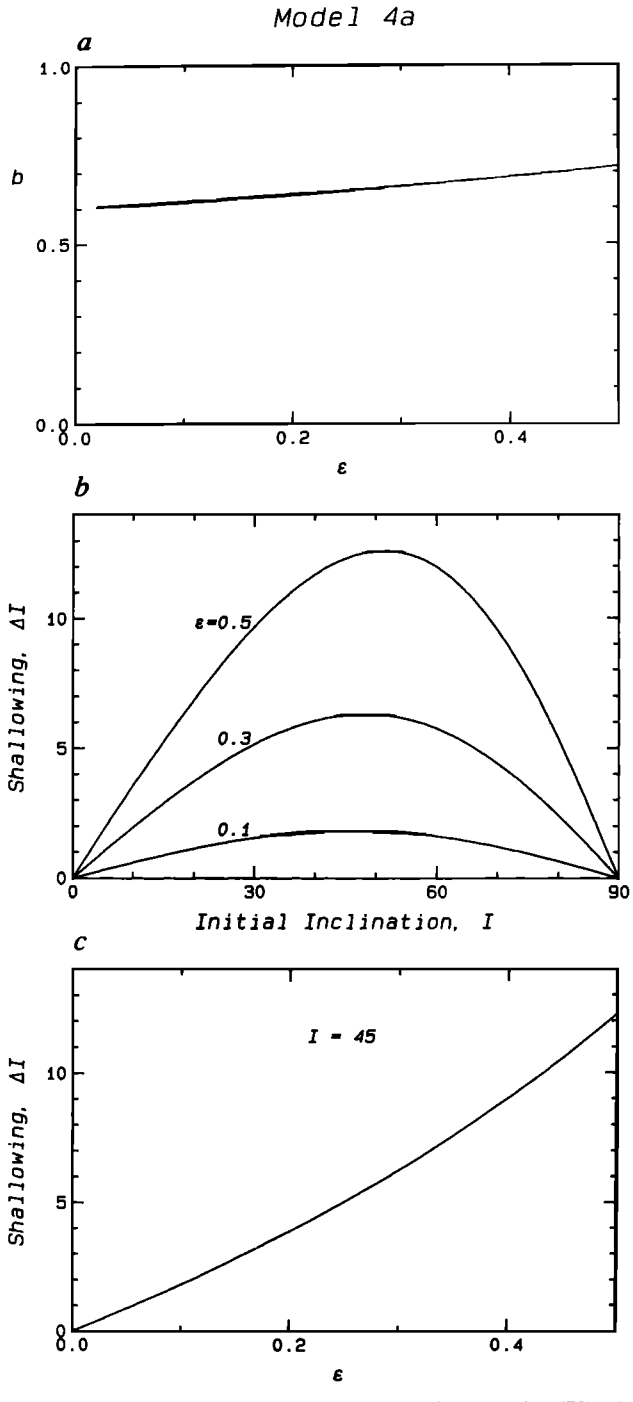

Fig. 12. Model 4a, initial within-sample dispersion, equation (73). (*a*) The function b as a function of ε, (b turns out to be close to a constant $b \approx 0.65$). (*b*) The inclination shallowing ΔI (deg), versus initial inclination I (deg) for various $\varepsilon = 0.1, 0.3, 0.5$. (*c*) The inclination shallowing ΔI (deg) versus ε, for initial inclination $I = 45°$. The effect of initial dispersion on a sediment that on a microscopic level satisfies $\tan(I - \Delta I) = (1 - \varepsilon)\tan I$ is to make it appear macroscopically to satisfy $\tan(I - \Delta I) = (1 - b\varepsilon)\tan I$.

where the special functions $\boldsymbol{K}$ and $\boldsymbol{E}$ are the complete elliptic integrals of the first and second kind, respectively. For compaction values between 0 and 0.5 ($\varepsilon = \Delta V$ for model 1a) we can approximate b' in equation (76) by

$$b' \approx 1.43 - 0.66\,\Delta V \tag{77}$$

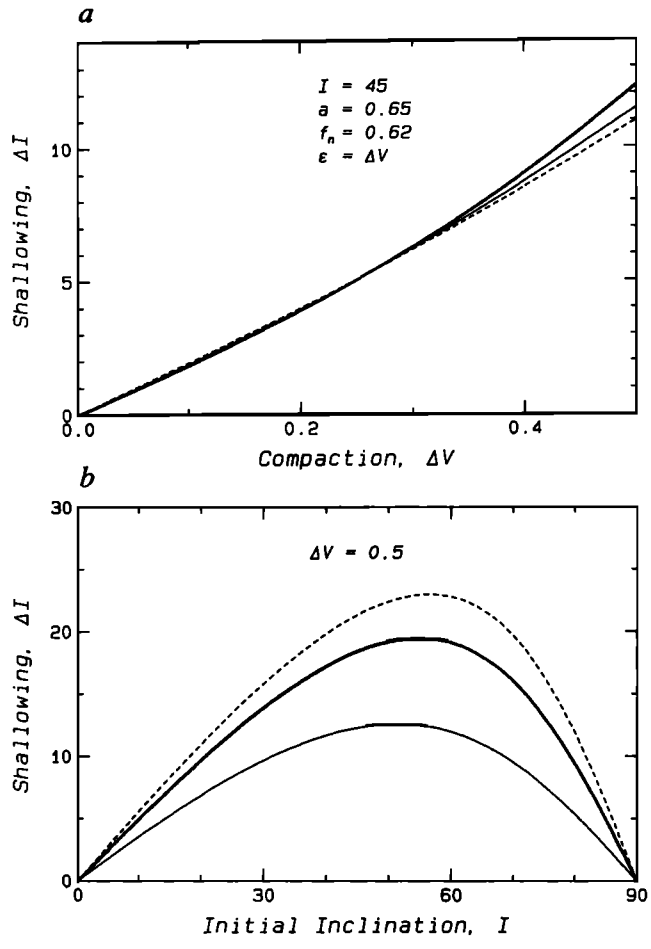

Fig. 13. Comparison of the predicted inclination shallowing of some of the models. (*a*) Comparison of model 1b (bold line), equation (18) when model 4a, equation (72) with $\varepsilon = \Delta V$, has been taken into account, model AK (dashed line), equation (8) with $a = 0.65$, and model 1c (solid line), equation (24) with $f_n = 0.62$, all for initial inclination of $I = 45°$. We note that the predictions of these models are very similar. (*b*) Comparison of macroscopic predictions of models 1a (dotted curve) and model 1b (dashed), when the effect of initial within-sample dispersion (model 4a) has been taken into account. For reference we also show the microscopic form of model 1b (solid), equation (18), when the effect of model 4a has not been taken into account. All curves are for compaction values $\Delta V = 0.5$, where $b = 0.716$ and $b' = 1.123$ (from the exact equations (74) and (76), respectively).

One remarkable result of the derivation in the appendix is that for the assumed form of the initial within-sample dispersion, we will obtain macroscopically an equation of the form

$$\tan(I - \Delta I) = (1 - F)\tan I \tag{78}$$

independent of the form of the equation of the microscopic mechanism responsible for the inclination shallowing. The microscopic mechanism serves only to define the function F. The effects of the expected initial within-sample dispersion on the models discussed in this paper will be to dampen the resultant inclination shallowing in equations (18), (22), (32), (37), (40), and (62) according to equation (73). This effect transforms the different form of equation (9) of model 1a to this standard form, with the modifying constant b' instead of b. We compare the transformed versions of models 1a and 1b in Figure 13*b*. The effect of initial dispersion should also affect equations (2), (6), (7), and (8), even though one may say that it is built in equation (8). Because of the

low initial alignment in natural sediments, the intensity variation in equations (41), (52), and (63) should be nearly independent of the initial inclination I. In these equations, I should be replaced by the effective average inclination I_{eff} which is constant about 30° (the average I over positive inclinations, weighted by the area of the directional sphere (cos I)). In equation (23) the correction factor c, should also be nearly independent of I, which makes it still closer to unity and it can probably be omitted in practical situations.

CONCLUSIONS

We have shown three possible mechanisms for inclination shallowing and a fourth process dampening the effect of all the other models slightly. The described models are realistic to different degrees. It is not usually known to what extent the magnetic minerals rotate directly, or whether they are attached to fabric flakes and are rotated through fabric rearrangements of the sedimentary matrix. Our calculations show that fabric rearrangement can not be a major source of inclination shallowing or intensity decrease. Sometimes deep-sea sediments show intensity decrease downhole, in otherwise homogeneous sections. Neglecting chemical alterations, this can be explained by directional randomization of the magnetic grains. The dispersion of magnetic moments predicted by the collapsing fabric, reduces the intensity less than the increased concentration due to compaction, and therefore leads to an intensity increase (Figure 8). In contrast, the randomization models readily predict the intensity decrease and in addition some inclination shallowing. We are therefore inclined to favor random rolling of sediment grains about horizontal axes as a significant process in sediments, leading to intensity decrease and inclination shallowing. The dampening of the inclination shallowing predicted by considering the effect of initial within-sample dispersion of moments is inevitable, and we believe that it has to be taken into account in all inclination shallowing models.

Studies of the fabric of clay rich sediments indicate that near the surface, the clay flakes are more or less randomly oriented, but compaction tends to collapse the matrix and reorient the particles to lie down with their flat surface horizontal [*Bennett et al.*, 1981]. Clay flakes have been reported to rearrange to nearly-horizontal orientations at depths of about 100 m in clay-rich deep-sea sediments [*Faas and Crocket*, 1983].

We have not been concerned with geochemical processes and possible dissolution of the magnetic grains in this paper, even though dissolution may be responsible for significant intensity decreases in some sediments [*Karlin and Levi*, 1985]. Neither have we addressed the effect of grain size. It is possible that in the randomization models larger grains may be less affected than the smaller ones. However, the grain size dependence is diminished whenever the magnetic grains are immobilized by being attached to larger fabric grains, because the matrix grains are usually considerably larger than the particles responsible for the stable remanence in sediments.

Inclination shallowing due to sediment compaction is clearly of great concern for paleomagnetism and the interpretation of paleomagnetic data. In this study we introduce simple mechanical models to derive mathematical expressions for the inclination shallowing during sediment compaction. We believe that all the models represent realistic physical processes active in sediments (except for model 1a at high values of I). The relative importance of the different mechanisms depends on the nature of the sediment and cannot yet be predicted a priori. However, several or all the processes may be active in any compacting sedimentary environment. In Table 1 we summarize the equations for the inclination shallowing models, taking into account the effect of initial within-sample dispersion (model 4a). We note the parallel structure of the equations, which arises because model 4a transforms any microscopic mechanism into this macroscopic form.

If a mechanism obeying the equation $\tan(I-\Delta I)= (1-p\Delta V)\tan I$ is followed by another mechanism obeying $\tan(I-\Delta I) = (1-q\Delta V)\tan I$, they will together result in $\tan(I-\Delta I) = (1-p\Delta V)(1-q\Delta V)\tan I \approx (1-(p+q)\Delta V)\tan I$. Therefore, until there is more specific knowledge of inclination shallowing

TABLE 1. Summary of the Equations of the Inclination Shallowing Models

Model	Author(s)	Equation of Model	Equation Number in Text
		Previously published models:	
K	[*King*, 1955]	$\tan(I-\Delta I) = (1-f_K)\tan I$	(2)
GKRW	[*Griffiths et al.*, 1960]	$\tan(I-\Delta I) = (1-f_G)\tan I$	(6)
BH	[*Blow and Hamilton*, 1978]	$\tan(I-\Delta I) = (1-\Delta V)\tan I$	(7)
AK	[*Anson and Kodama*, 1987]	$\tan(I-\Delta I) = (1-a\,\Delta V)\tan I$	(8)
		Models of this study: *	
1a: Rotating magnetic needles in rigid matrix		$\tan(I-\Delta I) = (1-b'\Delta V)\tan I$	(9)
1b: Rotating magnetic needles in soft matrix		$\tan(I-\Delta I) = (1-b\,\Delta V)\tan I$	(18)
1c: Two types of magnetic grain shapes in soft matrix		$\tan(I-\Delta I) = (1-b\,c\,f_n\Delta V)\tan I$	(22)
2a: Collapsing rigid matrix		$\tan(I-\Delta I) = (1-bf_a)\tan I$	(37)
2b: Collapsing soft matrix		$\tan(I-\Delta I) = (1-bf_b)\tan I$	(40)
3b: Random rolling of grains about horizontal axes		$\tan(I-\Delta I) = (1-bf_h)\tan I$	(62)

* The effects of model 4a, equation (73), are included in all the models of this study. The functions (nearly constants) b and b' are given in equations (75) and (77).

mechanisms in sediments, we recommend the use of an equation of the form

$$\tan (I - \Delta I) = (1 - a \Delta V) \tan I \quad (79)$$

where I is the ambient field inclination, ΔI the inclination shallowing, ΔV the compaction, and a is a constant, chosen to fit inclination shallowing data from laboratory experiments and natural sediments.

Appendix: Solutions to Some Calculus Problems

Collapsing Rigid Matrix

We want to find the exact mathematical solution to

$$F(\Delta V) = \int_0^{\pi/2} \cos \Delta\theta \; P_f(\theta) \; d\theta \quad (A1)$$

where $\Delta\theta$ is related to θ and ΔV by

$$\sin (\theta - \Delta\theta) = (1 - \Delta V) \sin \theta \quad (A2)$$

and the normalized probability distribution $P_f(\theta)$ is described by

$$P_f(\theta) \, d\theta = \sin \theta \, d\theta \quad (A3)$$

a distribution which describes a spherically random fabric flakes. Equation (A2) can be written with $\Delta\theta$ isolated

$$\Delta\theta = \theta - \arcsin ((1 - \Delta V) \sin \theta) \quad (A4)$$

We define for ease $a \equiv (1 - \Delta V)$, and now we can write

$$\cos \Delta\theta = \cos [\theta - \arcsin (a \sin \theta)] \quad (A5)$$

and this can be split, using the angle difference relation, to yield

$$\cos \Delta\theta = \cos \theta \cos [\arcsin (a \sin \theta)] + \sin \theta \sin [\arcsin(a \sin \theta)] \quad (A6)$$

which can be simplified to

$$\cos \Delta\theta = \cos \theta \sqrt{1 - a^2 \sin^2 \theta} + a \sin^2 \theta \quad (A7)$$

We can therefore write equation (A1) on the form

$$F(\Delta V) = \int_0^{\pi/2} [\cos \theta \sqrt{1 - a^2 \sin^2 \theta} + a \sin^2 \theta] \sin \theta \; d\theta \quad (A8)$$

this can be split into two integrals, and the first one simplified by the substitution

$$s \equiv \sqrt{1 - a^2 \sin^2 \theta} \quad (A9)$$

So we can write equation (A8) as

$$F(\Delta V) = -a^{-2} \int_1^{\sqrt{1-a^2}} s^2 \, ds + a \int_0^{\pi/2} \sin^3 \theta \, d\theta \quad (A10)$$

and the exact solution to equation (A1) assuming (A2) is

$$F(\Delta V) = [1 - (1 - a^2)^{3/2}] / [3 a^2] + 2 a / 3 \quad (A11)$$

or written out in full with ΔV

$$F(\Delta V) = 1 - \frac{(2 \Delta V - \Delta V^2)^{3/2} - 3 \Delta V^2 + 2 \Delta V^3}{3 - 6 \Delta V + 3 \Delta V^2} \quad (A12)$$

this result is used in equation (36).

Collapsing Soft Matrix

We want to find the exact mathematical solution to (A1) assuming now that $\Delta\theta$ can be connected to θ and ΔV by

$$\tan (\theta - \Delta\theta) = (1 - \Delta V) \tan \theta \quad (A13)$$

As before we define the variable $a \equiv (1 - \Delta V)$. From equation (A13) we can now write

$$\cos \Delta\theta = \cos [\theta - \arctan (a \tan \theta)] \quad (A14)$$

using now the angle difference relation, as before, we get

$$\cos \Delta\theta = \cos \theta \cos [\arctan (a \tan \theta)] + \sin \theta \sin [\arctan (a \tan \theta)] \quad (A15)$$

This can be simplified by standard relationships between $\sin x$, $\cos x$, $\tan x$, and $\arctan x$ [*Beyer*, 1984, pp. 139-140]. We are only interested in the first quadrant $0 \le x \le \pi/2$, where the trigonometric functions are positive, so we do not have to worry about sign problems. We define $t \equiv \tan \theta$.

Equation (A15) is now simplified to

$$\cos \Delta\theta = \frac{1}{\sqrt{1 + t^2}} \frac{1}{\sqrt{1 + a^2 t^2}} + \frac{t}{\sqrt{1 + t^2}} \frac{at}{\sqrt{1 + a^2 t^2}} \quad (A16)$$

or

$$\cos \Delta\theta = \frac{(1 + a t^2)}{\sqrt{(1 + t^2) (1 + a^2 t^2)}} \quad (A17)$$

and we can write $P_f(\theta)$ from equation (A3) as

$$\sin \theta = \frac{t}{\sqrt{1 + t^2}} \quad (A18)$$

By getting rid of $\Delta\theta$ we have now simplified equation (A1) to

$$F(\Delta V) = \int_0^{\pi/2} \frac{(1 + a \tan^2 \theta) \tan \theta}{(1 + \tan^2 \theta) \sqrt{1 + a^2 \tan^2 \theta}} d\theta \quad (A19)$$

in solving equation (A19) it is convenient to make the substitution

$$s \equiv \sqrt{1 + a^2 \tan^2 \theta} \quad (A20)$$

which transforms equation (A19) to

$$F(\Delta V) = \int_1^{\infty} \frac{a (s^2 - (1-a))}{(s^2 - (1-a^2))^2} \, ds \quad (A21)$$

This can be solved by using standard integral tables [e.g., *Beyer*, 1984, pp. 240-241, integrals 61a, 65, and 69, with $b = 1$, and $m = 1$]. We can now evaluate the integrals

$$g_1 = \int_1^\infty \frac{ds}{s^2-(1-a^2)} = \frac{1}{2\sqrt{1-a^2}} \ln\left(\frac{1+\sqrt{1-a^2}}{1-\sqrt{1-a^2}}\right) \quad \text{(A22)}$$

$$g_2 = \int_1^\infty \frac{ds}{(s^2-(1-a^2))^2} = \frac{1-a^2 g_1}{2a^2(1-a^2)} \quad \text{(A23)}$$

$$g_3 = \int_1^\infty \frac{s^2\, ds}{(s^2-(1-a^2))^2} = \frac{1+a^2 g_1}{2a^2} \quad \text{(A24)}$$

and write the solution to equation (A21)

$$F(\Delta V) = -a(1-a)\, g_2 + a\, g_3 \quad \text{(A25)}$$

Written out in full, the exact mathematical solution to equation (A1), assuming (A13) is then

$$F(\Delta V) = \frac{1}{2(2-\Delta V)} + \frac{(2-\Delta V)^2 - 1}{4(2-\Delta V)\sqrt{\Delta V(2-\Delta V)}} \ln\left(\frac{1+\sqrt{\Delta V(2-\Delta V)}}{1-\sqrt{\Delta V(2-\Delta V)}}\right) \quad \text{(A26)}$$

This result is used in equation (39).

Initial Within-Sample Dispersion

We want to solve

$$\tan(I-\Delta I) = \frac{\int_{-\pi/2}^{\pi/2}\int_0^{2\pi} \cos i\ (1+\kappa\cos\theta)\sin(i-\Delta i)\ dd\, di}{\int_{-\pi/2}^{\pi/2}\int_0^{2\pi} \cos i\ (1+\kappa\cos\theta)\cos(i-\Delta i)\ \cos d\ dd\, di} \quad \text{(A27)}$$

where θ is related to I, i, and d through

$$\cos\theta = \sin I \sin i + \cos I \cos i \cos d \quad \text{(A28)}$$

For convenience we define Z, and X

$$Z \equiv \int_{-\pi/2}^{\pi/2}\int_0^{2\pi} \cos i\ (1+\kappa\cos\theta)\sin(i-\Delta i)\ dd\, di \quad \text{(A29)}$$

$$X \equiv \int_{-\pi/2}^{\pi/2}\int_0^{2\pi} \cos i\ (1+\kappa\cos\theta)\cos(i-\Delta i)\ \cos d\ dd\, di \quad \text{(A30)}$$

and by applying equation (A28) in (A29) and (A30) we get

$$Z = \int_{-\pi/2}^{\pi/2}\int_0^{2\pi} [\cos i\ (1+\kappa\sin I\sin i)\sin(i-\Delta i)]\, dd\, di + \int_{-\pi/2}^{\pi/2}\int_0^{2\pi} [\cos i\ (\kappa\cos I\cos i)\sin(i-\Delta i)]\cos d\, dd\, di \quad \text{(A31)}$$

$$X = \int_{-\pi/2}^{\pi/2}\int_0^{2\pi} [\cos i\ (1+\kappa\sin I\sin i)\cos(i-\Delta i)]\cos d\ dd\, di + \int_{-\pi/2}^{\pi/2}\int_0^{2\pi} [\cos i\ (\kappa\cos I\cos i)\cos(i-\Delta i)]\cos^2 d\ dd\, di \quad \text{(A32)}$$

Integration over d from 0 to 2π is now a simple task and Z and X can be simplified to

$$Z = 2\pi\kappa\sin I \int_{-\pi/2}^{\pi/2} \cos i\ \sin i \sin(i-\Delta i)\, di \quad \text{(A33)}$$

$$X = \pi\kappa\cos I \int_{-\pi/2}^{\pi/2} \cos^2 i\ \cos(i-\Delta i)\, di \quad \text{(A34)}$$

The integrals in equations (A33) and (A34) are over symmetric functions about zero and can be replaced by double the integrals from 0 to $\pi/2$. At this point we notice that equation (A27) will take the form

$$\tan(I-\Delta I) = (1-F)\tan I \quad \text{(A35)}$$

where

$$F = 1 - \frac{2\int_0^{\pi/2} \cos i\ \sin i \sin(i-\Delta i)\, di}{\int_0^{\pi/2} \cos^2 i\ \cos(i-\Delta i)\, di} \quad \text{(A36)}$$

Equation (A35) carries great significance: We have not yet, in this derivation, introduced a microscopic relation defining the dependence of Δi on i and ε (or ΔV). Still we get the functional relationship of equation (A35). We have, in fact, shown that if the within-sample magnetic moments have dispersed orientations, the macroscopic relationship will take the form shown in equation (A35), independent of the form of the microscopic relationship between ΔI and ΔV. We note that F is a function of ε but independent of κ and I.

Now we connect $(i-\Delta i)$ to i and ε by

$$\tan(i-\Delta i) = (1-\varepsilon)\tan i \quad \text{(A37)}$$

and use the relations $\sin x = \tan x / (1+\tan^2 x)^{1/2}$ and $\cos x = 1/(1+\tan^2 x)^{1/2}$ to obtain

$$\sin(i-\Delta i) = (1-\varepsilon)\tan i / (1+(1-\varepsilon)^2\tan^2 i)^{1/2} \quad \text{(A38)}$$

$$\cos(i-\Delta i) = 1/(1+(1-\varepsilon)^2\tan^2 i)^{1/2} \quad \text{(A39)}$$

We define $\beta \equiv (1-\varepsilon)$, and Z' and X'

$$Z' \equiv 2\beta \int_0^{\pi/2} \sin^2 i \,/\, (1+\beta^2\tan^2 i)^{1/2}\, di \quad \text{(A40)}$$

$$X' \equiv \int_0^{\pi/2} \cos^2 i \,/\, (1+\beta^2\tan^2 i)^{1/2}\, di \quad \text{(A41)}$$

and these give the relation $\tan(I-\Delta I) = (Z'/X')\tan I$. Here it turns out to be convenient to use the substitution $s \equiv 1+\tan^2 i$, which transforms equations (A40) and (A41) to

$$Z' = 4\beta \int_1^{\infty} (s-1)/(s^2 A^{1/2})\, ds \quad \text{(A42)}$$

$$X' = 2 \int_1^{\infty} 1/(s^2 A^{1/2})\, ds \quad \text{(A43)}$$

where $A \equiv (\beta^2-1)+(1-2\beta^2)s+\beta^2 s^2$. These integrals can be solved using integral tables [e.g., *Beyer*, 1984, integrals 259 and 261, p. 257] resulting in

$$Z' = 2\beta\,[\arcsin(1-2\beta^2)+\pi/2]/(1-\beta^2)^{3/2} - 4\beta^2/(1-\beta^2) \quad \text{(A44)}$$

$$X' = (1-2\beta^2)[\arcsin(1-2\beta^2)+\pi/2]/(1-\beta^2)^{3/2} + 2\beta/(1-\beta^2) \quad \text{(A45)}$$

And finally we define the function b such that $(1-b\varepsilon) = Z'/X'$, incorporate relationships between arcsin and arccos, and replace β by $(1-\varepsilon)$ to get

$$(1-b\varepsilon) = \frac{2(1-\varepsilon)\arccos(1-4\varepsilon+2\varepsilon^2) - 4(1-\varepsilon)^2\sqrt{2\varepsilon-\varepsilon^2}}{-(1-4\varepsilon+2\varepsilon^2)\arccos(1-4\varepsilon+2\varepsilon^2) + 2(1-\varepsilon)\sqrt{2\varepsilon-\varepsilon^2}} \quad \text{(A46)}$$

This result is used in equation (74).

To calculate the effect of initial within-sample dispersion on model 1a, we have to start form equation (A35) and (A36), and instead of equation (A37), we connect $(i-\Delta i)$ to i and ε by

$$\sin(i-\Delta i) = (1-\varepsilon)\sin i \quad \text{(A47)}$$

and use the relation $\cos x = (1-\sin^2 x)^{1/2}$ to obtain

$$\cos(i-\Delta i) = (1-(1-\varepsilon)^2\sin^2 i)^{1/2} \quad \text{(A48)}$$

As before we define $\beta \equiv (1-\varepsilon)$, and Z' and X'

$$Z' \equiv 2\beta \int_0^{\pi/2} \cos i \,\sin^2 i\, di \quad \text{(A49)}$$

$$X' \equiv \int_0^{\pi/2} \cos^2 i\,(1-\beta^2\sin^2 i)^{1/2}\, di \quad \text{(A50)}$$

and these give the relation $\tan(I-\Delta I) = (Z'/X')\tan I$. Equation (A49) is easily solved to give $Z' = 2(1-\varepsilon)/3$. However, equation (A50) is an elliptic integral, which can not be written in terms of elementary functions, but can be written in terms of the special functions $\boldsymbol{K}(k)$ and $\boldsymbol{E}(k)$, called the complete elliptic integrals of the first ($\boldsymbol{K}$) and second ($\boldsymbol{E}$) kind [*Gradshteyn and Ryzhik*, 1980, integral 2.583.6, p. 159]. For model 1a we define $(1-b'\varepsilon) \equiv (Z'/X')$, which can be written as

$$(1-b'\varepsilon) = \frac{2(1-\varepsilon)^3}{((1-\varepsilon)^2-1)\boldsymbol{K}(1-\varepsilon) + ((1-\varepsilon)^2+1)\boldsymbol{E}(1-\varepsilon)} \quad \text{(A51)}$$

This result is used in equation (76).

Acknowledgments. We thank P. Roperch, K. Kodama, and an anonymous reviewer for constructive comments. This work was supported by the National Science Foundation and the Icelandic Government Student Loan Fund.

References

Anson, G. L., and K. P. Kodama, Compaction-induced shallowing of the post-depositional remanent magnetization in a synthetic sediment, *Geophys. J. R. Astron. Soc.*, *88*, 673-692, 1987.

Arason, P., and S. Levi, Inclination shallowing recorded in some deep sea sediments (abstract), *Eos Trans. AGU*, *67*, 916, 1986.

Bennett, R. H., W. R. Bryant, and G. H. Keller, Clay fabric of selected submarine sediments: Fundamental properties and models, *J. Sediment. Petrol.*, *51*, 217-232, 1981.

Beyer, W. H. (Ed.), *CRC Standard Mathematical Tables*, 27th ed., 615 pp., CRC Press, Boca Raton, Fla., 1984.

Blow, R. A., and N. Hamilton, Effect of compaction on the acquisition of a detrital remanent magnetization in fine-grained sediments, *Geophys. J R. Astron. Soc.*, *52*, 13-23, 1978.

Celaya, M. A., and B. M. Clement, Inclination shallowing in deep sea sediments from the North Atlantic, *Geophys. Res. Lett.*, *15*, 52-55, 1988.

Chikazumi, S., *Physics of Magnetism*, 554 pp., John Wiley, New York, 1964.

Collinson, D. W., Depositional remanent magnetization in sediments, *J. Geophys. Res.*, *70*, 4663-4668, 1965.

Faas, R. W., and D. S. Crocket, Clay fabric development in a deep-sea core: Site 515, Deep Sea Drilling Project leg 72, *Initial Rep. Deep Sea Drill. Proj*, *72*, 519-535, 1983.

Fisher, R., Dispersion on a sphere, *Proc R. Soc. London, Ser. A*, *217*, 295-305, 1953.

Gradshteyn, I. S., and I. M. Ryzhik, *Table of Integrals, Series, and Products*, 1160 pp., 4th ed., Academic, San Diego, Calif., 1980.

Griffiths, D. H., R. F. King, A. I. Rees, A. E. Wright, Remanent magnetism of some recent varved sediments, *Proc. R. Soc. London, Ser. A*, *256*, 359-383, 1960.

Hamilton, E. L., Thickness and consolidation of deep-sea sediments, *Geol. Soc. Am. Bull.*, *70*, 1399-1424, 1959.

Karlin, R., and S. Levi, Preliminary paleomagnetic results of laminated sediments from deep sea drilling project hydraulic piston core site 480, Guaymas basin, Gulf of California, *Initial Rep. Deep Sea Drill. Proj.*, *64*, 1255-1258, 1982.

Karlin, R., and S. Levi, Geochemical and sedimentological control of the magnetic properties of hemipelagic sediments, *J. Geophys. Res.*, *90*, 10,373-10,392, 1985.

Kent, D. V., Post-depositional remanent magnetization in deep-sea sediment, *Nature*, *246*, 32-34, 1973.

Kent, D. V., and D. J. Sparíosu, Magnetostratigraphy of Caribbean site 502 Hydraulic Piston Cores, *Initial Rep Deep Sea Drill. Proj.*, *68*, 419-433, 1982.

Khramov, A. N., Orientational magnetization of finely dispersed sediments, *Izv. Acad. Sci. USSR Phys. Solid Earth*, *1*, 63-66, 1968.

King, R. F., Remanent magnetism of artificially deposited sediments, *Mon. Not. R. Astron. Soc., Geophys. Suppl.*, *7*, 115-134, 1955.

Langevin, P., Magnétisme et théorie des électrons (in French), *Ann. Chim. Phys.*, *5*, 70-127, 1905.

Levi, S., and R. T. Merrill, Properties of single-domain, pseudo-single-domain, and multidomain magnetite, *J. Geophys. Res.*, *83*, 309-323, 1978.

Mardia, K. V., *Statistics of Directional Data*, 357 pp., Academic, San Diego, Calif., 1972.

Morgan, G. E., Paleomagnetic results from DSDP site 398, *Initial Rep. Deep Sea Drill. Proj.*, *47*, 599-611, 1979.

Nagata, T., Notes on detrital remanent magnetization of sediments, *J. Geomagn. Geoelectr.*, *14*, 99-106, 1962.

Nobes, D. C., H. Villinger, E. E. Davis, and L. K. Law, Estimation of marine sediment bulk physical properties at depth from seafloor geophysical measurements, *J. Geophys. Res.*, *91*, 14,033-14,043, 1986.

Ozima, M., Effects of plastic deformation on the remanent magnetization of a Cu-Co alloy, *Earth Planet. Sci. Lett.*, *47*, 121-123, 1980.

Stacey, F. D., On the role of Brownian motion in the control of detrital remanent magnetization of sediments, *Pure Appl. Geophys.*, *98*, 139-145, 1972.

Stober, J. C., and R. Thompson, Magnetic remanence acquisition in Finnish lake sediments, *Geophys. J. R. Astron. Soc.*, *57*, 727-739, 1979.

Tauxe, L., P. Tucker, N. P. Petersen, and J. L. LaBrecque, Magnetostratigraphy of leg 73 sediments, *Initial Rep. Deep Sea Drill. Proj.*,*73*, 609-621, 1984.

Tomlinson, M. J., *Foundation Design and Construction*, 793 pp., 4th ed., Pitman Advanced Publishing Program, Boston, Mass., 1980.

Tschebotarioff, G. P., *Soil Mechanics, Foundations and Earth Structures*, 655 pp., McGraw-Hill, New York, 1951.

Tucker, P., Stirred remanent magnetization: A laboratory analogue of post-depositional realignment, *J. Geophys.*, *48*, 153-157, 1980.

Verosub, K. L., Depositional and postdepositional processes in the magnetization of sediments, *Rev. Geophys.*, *15*, 129-143, 1977.

Von Mises, R., Über die "ganzzahligkeit" der atomgewichte und verwandte fragen (in German), *Phys. Z.*, *19*, 490-500, 1918.

P. Arason and S. Levi, Geophysics, College of Oceanography, Oregon State University, Oceanography Admin Bldg 104, Corvallis OR 97331-5503.

(Received September 30, 1988;
revised October 5, 1989;
accepted October 16, 1989.)